This is to certify that the

thesis entitled

A PROCEDURE FOR THE DYNAMIC INVESTIGATION
OF HUMAN GAIT

presented by

Trena Lynn Markus

has been accepted towards fulfillment
of the requirements for

M.S. degree in Mechanics

Major professor

Date February 17, 1986

A PROCEDURE FOR THE DYNAMIC INVESTIGATION OF HUMAN GAIT

By

Trena Lynn Markus

A THESIS

Submitted to
Michigan State University
in partial fullfillment of the requirements
for the degree of

MASTER OF SCIENCE

Department of Metallurgy, Mechanics and Material Science

1986

ABSTRACT

A PROCEDURE FOR THE DYNAMIC INVESTIGATION
OF HUMAN GAIT

By

Trena Lynn Markus

The purpose of this investigation was to develop a procedure for the computation of the dynamic parameters used in the description of human locomotion. The subject was filmed while running across a force platform to obtain lower limb position data. The lower limb was modeled as a two-dimensional system of articulating rigid linkages and the angular velocities, angular accelerations and the external joint forces and moments were calculated for each segment.

The force reactions at the three joints revealed little attenuation of forces in the vertical direction. Of the three joints, the greatest anterior/posterior forces were recorded at the hip. The moment reaction at the three joints indicated that in braking phase, peak moments were observed in the hip and knee while during propulsion stage, the ankle and hip moments achieve dominance.

To my dear husband Alan, for his endless understanding, encouragement and love during the completion of my graduate work.

ACKNOWLEDGMENTS

The author wishes to express her deepest appreciation to the following people for making the completion of her Master of Science degree possible:

To her major professor, Dr. Robert W. Soutas-Little, for his guidance, encouragement and friendship.

To Robert Schaeffer, for his assistance in equipment development and testing, as well as his endless patience.

To Michael H. Schwartz, for his constant assistance and perseverance, and, most of all, for his warm friendship.

To Brooks Shoe, Incorporated, for their generous funding of this project.

To Mary C. Verstraete, for her encouragement, support and warm friendship.

To Andrew Hull, for his valuable assistance in computer program development.

TABLE OF CONTENTS

LIST OF FIGURES

Figure | Page

I. INTRODUCTION

As a locomotive mechanism, the human body is, by far, the most complex "machine" ever designed. The body is supported by a superstructure of articulating limb segments. connected by several types of joints, thus providing a broad spectrum of different ranges of motion. These levers are powered by thousands of motor units which make up the muscles of the body. Connecting the muscle cells to the brain is a vast network of nerves responsible for initiating the muscle action. The electrically stimulated muscles cells contract, generating a force which results in motion of the limb segments. While this is a tremendously simplified view of the anatomical components necessary in human ambulation, it does indicate the multitude of events which must occur in order to produce even the simplest of movements.

The first attempt at quantifying human locomotion was published in the mid 1800's. Investigators soon realized the difficulty of describing human gait in analytical terms. The three dimensional motion requires complicated analysis, although restricting the investigation to the plane of progression simplifies the process and still yields a great deal of valuable information. Variations in skeletal size and musculature among subjects requires a method of external measurement to determine such values as mass moments of inertia, segment lengths and masses and center of mass locations. Perhaps the greatest challenge facing early gait investigators was the sheer number of calculations necessary in determining the dynamic parameters of locomotion. In their

1950 publication, Bresler and Frankel stated that for one stride, 14,000 numerical calculations were performed, 72 curves were plotted and 24 curves were subjected to graphic differentiation, requiring 500 man hours to complete (3).

The advent of the computer greatly reduced the amount of time spent on data analysis and the number of investigators interested in gait analysis increased dramatically. Studies have included the determination of ground reaction forces, joint forces and moments, energy and power flow in the segments and muscle force contributions. In the majority of these works, walking was the mode of gait studied, as it is the principal form of human locomotion. Analyzing the mechanical functions of the body of normal subjects while walking provides a baseline from which subjects with abnormal gait patterns can be compared. This is extremely useful in the diagnosis of injuries and joint deterioration, as well as in the design of prosthetic devices.

As indicated by the exponential growth in the number of participants in the Boston Marathon over the past two decades, running has become one of the most popular forms of exercise (4). An activity which was once limited to competing athletes is now an integral part of the daily routine for millions of fitness-conscious Americans yet, very few papers have been published regarding the kinetics of running. Investigating the dynamic parameters of running will provide a greater understanding of the relationship between running kinetics and kinematics. A dynamic analysis technique for running would enable investigations of the changes of these variables with running speed, running style, footwear and injury. The sheer number of running participants, as well as the sparsity of information available is justification for research in this area. Therefore, the purpose of this study was to develop a procedure to compute the dynamic parameters generated during the stance phase of running.

II. SURVEY OF LITERATURE

The vast amount of information available today regarding gait analysis is due to the contributions of many scientists. The majority of individuals mentioned here have limited their investigations to the subject of joint force and moment determination. In 1836, Wilhelm and Edward Weber introduced a model likening human gait motion to that of a pendulum, and concluded that during swing phase, the leg displayed pure pendulum motion and there was no muscular contribution during this period (20). This theory was later invalidated by a number of investigators. E.J. Marey performed a number of tests in the late 1800's to determine the center of pressure on the sole of the foot, energy outputs during locomotion and vertical displacement of the body during walking. His greatest contribution, however, was the development of chronophotography — a method of repeatedy exposing photographic film using a rotating disk (13). In 1872, Braune and Fischer submitted what is still considered a classical study of kinetic properties for different segments of the body (2).

The first attempt in determining the forces and moments generated in human locomotion was reported in 1939 by Herbert Elftman at Columbia University (8). Elftman successfully constructed a force platform capable of measuring the three components of force, as well as the points of force application. Using this device, in conjunction with chronophotographic techniques, Elftman was able to determine the two dimensional external joint forces and torques, as well as energy changes in the leg during walking. Vertical forces at all three joints exhibited a double peak pattern with maximum values slightly exceeding body weight. Fore-and-aft forces first resisted forward body motion and reversed direction at the approach of toe off. The sagittal moments varied in pattern among the three joints of interest. The ankle was dominated by a plantar flexor moment while the knee exhibited a slight flexion followed by extensor activity. The hip began with extensor activity followed by a flexor moment at midstance.

Bresler and Frankel continued Elftman's work in 1950 by considering a three-dimensional analysis of the lower limb while walking (3). The study was conducted using a force platform and a 35 mm motion picture camera to record the ground force and displacement data necessary for joint force and moment determination. The lateral components of the external joint forces during stance phase were found to be very small in magnitude when compared to the vertical and fore-and-aft components. The fore-and-aft components displayed a typical shape approximating a sine wave while the vertical components closely resembled the double peak pattern of the ground reaction. Examination of the moment patterns indicate the largest moment contributions were recorded about the lateral axis with a significant moment at the hip occurring about the fore-and-aft axis. Typical peak force and moment values occurred at the ankle; with a vertical force 1.2 times body weight and a moment about the medial-lateral axis of 102 Newton-meters.

In 1966, J.P. Paul studied the biomechanics of the hip joint by considering not only the forces and moments between the leg and the trunk, but also the joint forces between the acetabulum and the femoral head (15). The forces and moments between the leg and trunk were computed by considering the effects of gravity, acceleration and external forces and displayed trends similar to those described by Bresler and Frankel. The joint forces computation required the additional knowledge of the muscle forces acting at the hip and revealed a range of values from 2.3 to 5.8 times body weight with an average peak resultant value of 5.0. The results from this study are useful in fitting external prostheses as well as designing the components necessary in a total hip replacement.

J.B. Morrison developed experimental techniques to study the function of the knee joint during normal activities based on the methods used by Bresler and Frankel and J.P. Paul (3,15). The knee was modeled as a hinge joint acted upon by a reduced system comprised of the forces in three muscle groups and four ligaments and the external force system acting at knee joint. Electromyography was used to record periods of muscle activity and cadaver measurements were made to yield the magnitude and line of action for each muscle group. The resulting joint force revealed three main periods of peak loading, each attributed to the activity of one of the three muscle groups. The mean peak value recorded was 3.0 times body weight. The external force system acting at the knee joint showed good comparison with the results obtained by Bresler and Frankel.

Regardless of the method of measurement and data reduction, all kinematic acquisition techniques are susceptable to noise in the spatial information. In 1974, D. Winter, H.G. Sidwall and D.A. Hobson determined the frequency spectrum of the noise and spatial signal and developed a low pass digital filter to reduce the noise component (23). Using a Butterworth filtering technique, with a cutoff frequency at the seventh harmonic, velocity and acceleration information was obtained by direct digital differentiation of the position data.

In addition to filtering, the method of curve fitting or differentiation influences the accuracy of the resulting acceleration values. J.C. Pezzack, R.W. Norman and D.A. Winter compared analog acceleration signals with accelerations determined by finite differences, Chebyshev least squares polynomial curve fitting and digital filtering combined with finite difference techniques (16). The results strongly supported the procedure of filtering before using a finite difference method of differentiation as this most accurately reproduced the analog signal. In addition, this method is easily used and several cutoff frequencies may be tried to obtain the best fit.

In 1978, R.O. Crowninshield, R.C. Johnson, T.G. Andrews and R.A. Brand conducted a biomechanical investigation of the human hip during walking, rising and descending stairs and rising from a sitting position (6). Euler angle theory and force platform output were used to compute intersegmental resultant forces and optimization techniques distributed these resultants to twenty seven musculotendinous structures in the vicinity of the hip. This hip study compared well with Paul's 1966 investigation, with values ranging from 3.3 to 5 times body weight and an average of 4.3 for hip contact force. The hip resultant force components displayed trends typical of those seen in previous studies.

David A. Winter, dissatisfied with using moments of force as a description of the kinetic activity present during gait, described a new method of gait assessment in a 1980 publication (22). The principal of lower limb support states the algebraic summation of the net extensor moments at the ankle, knee and hip during stance phase must be positive to prevent total limb collapse. This theory was upheld by the moment patterns of 30 case studies, which were calculated using a procedure based on the Bresler and Frankel methods. In addition, it was determined that amputees, hemiplegics and knee replacement patients also exhibit this pattern demonstrating that the normally functioning joints compensate for the deficient joint.

In 1981, one of the few papers describing the kinetics of running was published by R.V. Mann (12). The two dimensional data was acquired for the ankle, knee, hip, elbow and shoulder using a filming force platform protocol as the runner exerted a maximum sprint effort. The moment about the ankle displayed a plantar flexor dominance during ground contact. The knee pattern during stance phase revealed a slight flexor activity followed by extensor dominance. The hip moment showed an extensor to flexor dominance during ground contact. The greatest effort was seen at the point just after foot strike when the hip extensor/knee flexor muscle group was dominate. The shoulder displayed flexor to extensor activity while the elbow was totally flexor dominated. The small magnitude of the upper limb moments indicated that the arms' primary purpose in running is to maintain balance.

A paper describing the moments of force generated during jogging was published by David A. Winter in 1983 (21). In addition, the support moment and the mechanical power generated and absorbed at each joint was determined. The moment patterns displayed points of maximum extension at 20%, 40% and 60% of stance for the hip, knee and ankle, respectively, and the sum of the extensors supported the theory of lower limb support. The power levels at the hip were small, while the major generation of energy occurred at the ankle with a minor contribution at the knee.

The use of accelerometers for kinematic data acquisition was reported in 1984 by J.A. Gilbert, G.M. Maxwell, J.H. McElhaney and F.W. Clippinger (9). The resulting accelerations, together with ground reaction forces obtained with force platform, were used to determine the forces and moments in the sagittal plane at the knee and hip. Peak accelerations between 1 and 2 g's were recorded at heel strike and force and moment values compared favorably with those reported by previous investigators. However, the plots contained a high frequency signal superimposed in the gross motion pattern that were attributed to inertial forces on the upper and lower leg masses.

e
c
p
a
r
f
c
r
c
t
w
s
(
e
f
w
r
t
a
t

III. EXPERIMENTAL METHODS

An experimental protocol and data acquisition system were established to obtain the kinematic parameters necessary in the computation of the joint forces and moments generated during the contact phase of normal gait. The procedure involved filming a subject striking a force platform using cine-photogrammetry techniques (1,19). Two Locam motor driven 16 mm cine-cameras operating at 100 frames/second were used to record position data for selected targets on the left leg. The two cameras were oriented such that each camera's field of view contained a rear and lateral view of the targeted area. The cameras' heights and distances were set so the targeted leg optimally filled the film frame to ease the task of digitizing. This system, developed by Dr. James Walton, does not require the cameras to be placed at right angles to the subject or one another, thus facilitating rapid and easy set up (18). Once positioned, the two cameras were coupled to a single switch, thus enabling the cameras to be turned on simultaneously. To synchronize the film data from each camera, a timing light box accurate to 1/1000 second was placed in each camera's field of view. The frame-by-frame time record was also useful in determining the time between foot strike and toe off. To complete the filming set up, additional lighting was arranged around the force platform to provide adequate illumination of the filming area (Figure 1).

Figure 1. FILMING SET-UP

The ground reaction forces exerted on the body were measured using a three-dimensional strain gage type force platform* mounted flush with the running surface. The strain gages, wired into a balanced four arm bridge, became unbalanced when a measureable strain was detected. The resulting voltage changes were processed by means of an amplifier, an A to D converter and an IBM 9000 computer. Six channels monitored the forces and moments in the three principal directions; X and Y being the horizontal axes and Z being the vertical axis (Figure 2). A seventh channel was used to monitor the timing lights, enabling the synchronization of the film and force data.

* Model OR6-3 Advanced Mechanical Technology 141 California Street, Newton, MA 02158

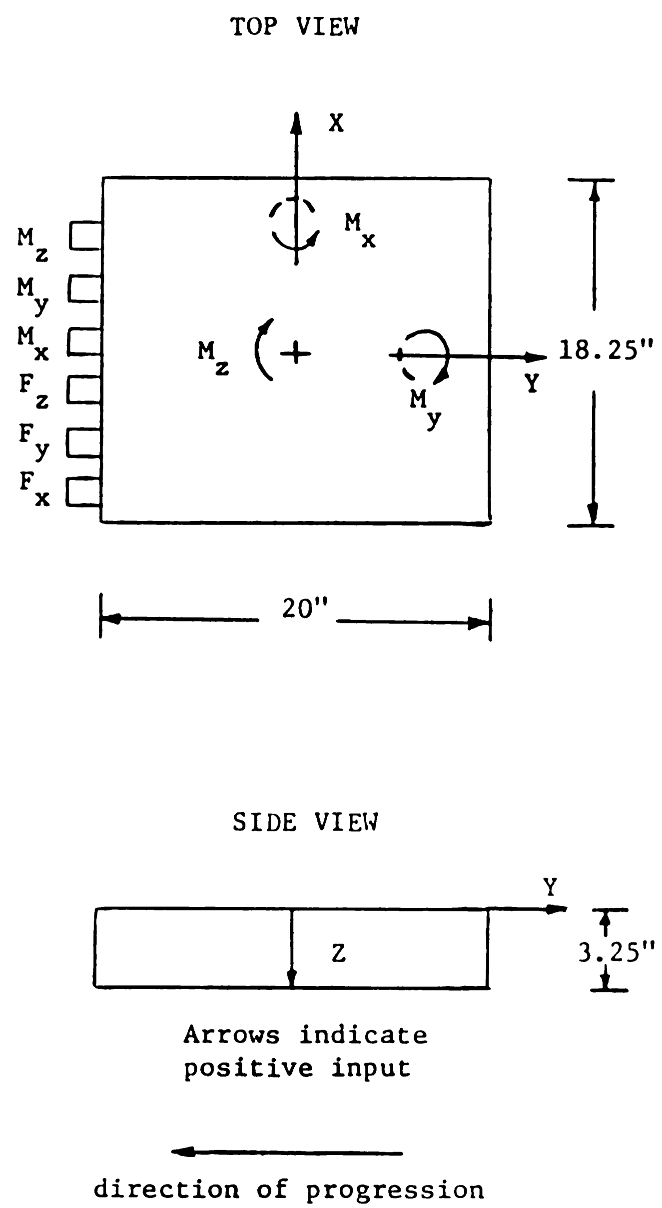

Figure 2. FORCE PLATFORM SIGN CONVENTION

A computer program* was utilized to sample, process and store data from the force platform using the IBM 9000 computer. Data sampling at a rate of one millisecond was initiated when an applied vertical load was detected and continued for 4 seconds following the threshold event. The loads were received as raw voltages and converted to equivalent mechanical units, with forces expressed in Newtons and moments in Newton-meters. The converted data was stored on an 8" floppy disk after each individual trial. Following the completion of all trials, hard copy of each event was obtained for the forces in the vertical and anterior-posterior directions in both tabular and graphical format.

The subject of this study was a 23 year old female running an average of 35 miles per week with a body weight of 130 lbs. The running shoe worn during testing was the Brooks Chicago Racer. Ten 1/2" orange yarn pompons were used to target specific locations on the left leg and shoe. The orange color provided good visibility while the size enabled ease in locating the center of the target during digitizing without being too large so as to cause the location to become arbitrary. All of the targets were fixed to the subject using ordinary rubber cement.

Four targets were used to define two theoretical rigid links to approximate the motion of the lower limb. The targets placed on the protuberance of the greater trochanter and the lateral condyle of the femur marked the endpoints of the upper link. The lower link was defined by targets placed on the lateral condyle of the tibia and the lateral malleolus of the ankle (Figure 3). The remaining six targets

* Mr. Fred Brunye and Mr. Robert Wells, 1983.

Figure 3. LOWER LIMB LINKAGE TARGETING

were arranged in two triads which were located on the shank and the shoe. The triads allowed the three dimensional motion of the foot about three body segment axes to be determined using a joint coordinate system (8). The shank triad was constructed from two targets positioned approximately three inches apart along the superior-inferior axis to the rear of the leg. The third target was located between the pair and rotated anteriorly and laterally before being fixed in position. The triad located on the shoe was oriented in a similar manner (Figure 4).

Following the application of the targets, calipers were used to measure the lateral-medial width of the body segments at targets C and F.

Figure 4. SHANK AND SHOE TRIAD TARGETING

Once targeted, the subject warmed up on a treadmill for several minutes. To insure that the runner strikes the platform without altering her stride, a piece of tape was place on the runway approximately 5 meters before the platform. The exact marker position was determined during practice runs to suit the subject's individual needs. An additional piece of tape was placed 10 meters from the first marker to aid in velocity determination. Two stop watches were used to measure the time elapsed as the subject passed between the markers and the subject's velocity was calculated and recorded. Since the particular area of interest of this study was distance running, a velocity range of 3.6 - 4.0 meters per second was chosen to simulate an approximate seven minute mile pace.

Prior to subject filming, a calibration structure with twelve previously located spheres was placed in the field of view of the cameras and filmed (1). The twelve predetermined targets set the matrix transformation constants necessary to determine the three dimensional coordinates of the body targets. The calibration structure was then removed and a number board identifying the date, the subject and the trial number was filmed before each trial. The subject ran at least three trials with additional trials added if the runner missed the platform or posted a velocity outside of the predetermined range. A mistrial was also declared if the subject felt her stride was unnatural or forced in any way. Finally, the calibration structure was placed in the field of view and refilmed as a precautionary measure. After being professionally processed, the film from each camera was spliced together and wound on one reel for frame by frame digitizing. Digitizing was accomplished using a Vanguard Motion Analyzer and a Sonic Digitizer. The twelve target points of the calibration structure were digitized first, followed by the side and rear views of the subject targets. Five frames before and after contact phase were also digitized to insure an adequate number of data points would be preserved following data differentiation and filtering. The occurrence times for foot strike, toe off, as well as the first and last frames digitized, were determined from the timing light configuration present in each frame and recorded. The times posted in corresponding rear and side frames were within 1/100 second and indicated good synchronization between the cameras. Both the calibration and subject data were stored in data files by means of a Decwriter connected by a modem to a Prime mainframe computer located at the A.H. Case Center for Computer-Aided Design. The position data points were determined using a series of computer programs which located the positions of the subject targets based on the transformation constants determined from the calibration data (19). The two dimensional data from each view was then combined and time-matched to obtain the three dimensional position information for the targeted locations on the subject's leg.

IV. ANALYTICAL METHODS

Following digitization, a series of computer programs were used to compute the dynamic parameters necessary in the determination of the joint forces and moments. The digitized position data were separated into linkage and triad data files and subjected to different methods of processing. The position data from the four linkage targets were subdivided into the three orthogonal directions to yield twelve storage files. The data held in these files were filtered and differentiated in accordance with the methods developed by Winter and co-workers to obtain the relative velocities and accelerations of the targeted body landmarks (23).

The filter*, based on Butterworth filtering techniques, was designed with a cutoff frequency of 10 Hertz (23). This frequency insured the preservation of gross body motion while removing electrical noise and other high frequency signals (Figure 5). The position data were filtered in forward sequence followed by reverse sequence to eliminate the phase lag commonly associated with Butterworth filters. The filtered data were then differentiated to obtain velocities using a three point forward difference approximation** (16). The accelerations were also determined from the filtered position data using a four point

* Mr. Andrew Hull, 1985
** Mr. Andrew Hull, 1985

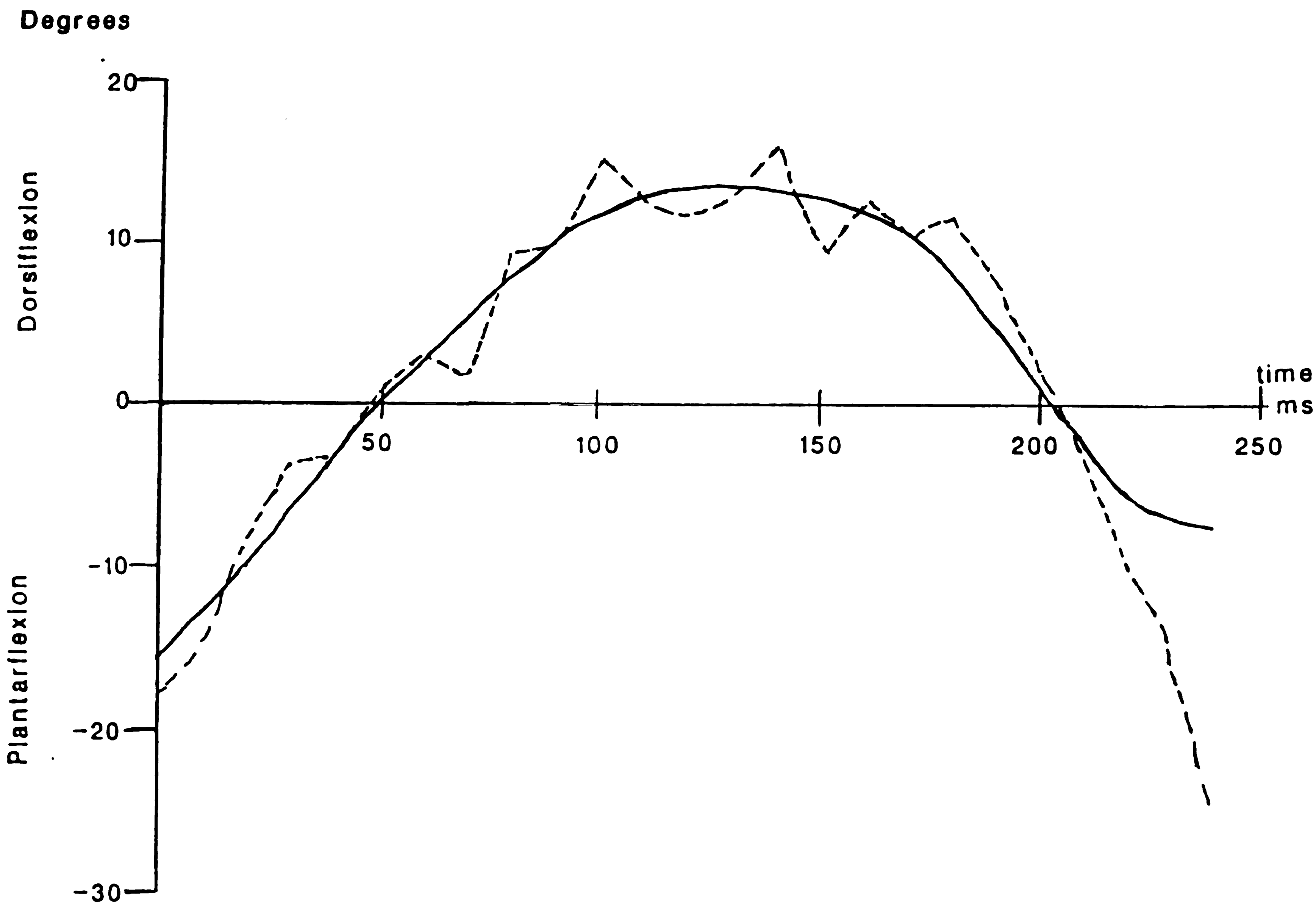

Figure 5. FILTERED VERSUS UNFILTERED ANGULAR DATA

forward difference method. All velocities and accelerations were stored in individual data files to facilitate future calculations.

The triad position data were processed using a computer program which determined the foot rotations based on the joint coordinate system method (10,18). Using the triad positions, the program computed a set of non-orthogonal body segment reference axes and measure the motion of the foot relative to the shank as rotations about these axes. Inversion and eversion was defined as a rotation about the $\hat{e}_1$ axis, plantar and dorsi flexion was a rotation about the $\hat{e}_2$ axis and medial and lateral rotation was a rotation about the $\hat{e}_3$ axis (Figure 6). The angular displacement curves were subjected to the same filtering and differentiating techniques outlined earlier in this chapter and the resulting angular velocities and accelerations were stored in data files.

To obtain the angular velocities and accelerations of the upper and lower linkages, the following equations were implemented based on the rigid body theory of motion.

$$(1) \qquad \vec{V}_B = \vec{V}_A + \vec{V}_{B/A} \quad \text{where } \vec{V}_{B/A} = \vec{\omega} \times \vec{r}$$

Where $\vec{V}_A$ and $\vec{V}_B$ are the velocities of points A and B, $\vec{V}_{B/A}$ is the velocity of B relative to A and $\vec{\omega}$ is the angular velocity of the linkage.

From the filtered and differentiated data, the velocities of points A and B were known. The radius vector, $\vec{r}$, between A and B was easily calculated by taking the difference between the A and B position coordinates.

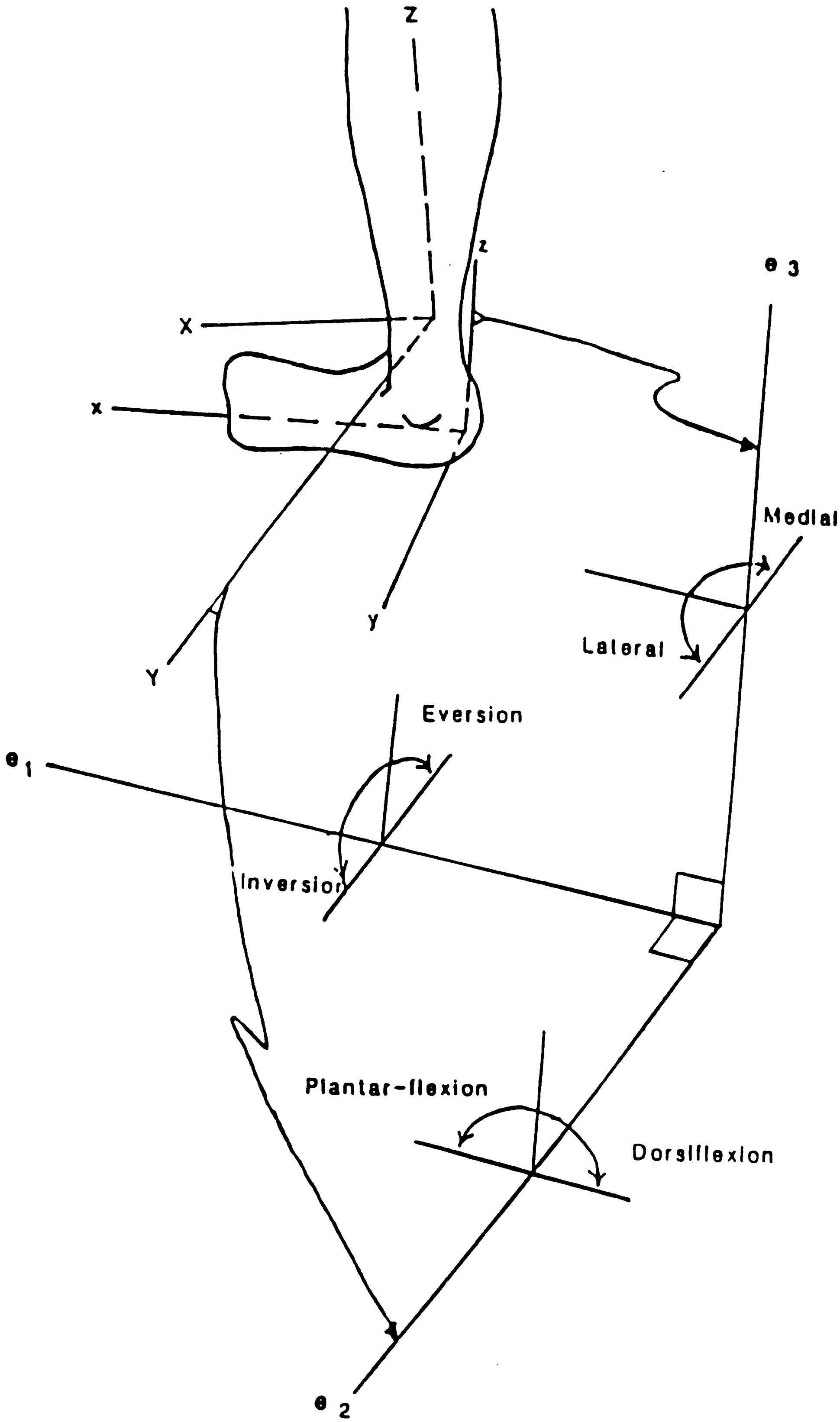

Figure 6. ORIENTATION OF THE JOINT COORDINATE SYSTEM

Rearranging the equation:

$$\vec{V}_B - \vec{V}_A = \vec{V}_{B/A} = \vec{\omega} \times \vec{r}$$

According to this equation, $\vec{V}_{B/A}$ is assumed to be perpendicular to the radius vector. However, due to the data processing and soft tissue motion, this criterion was not satisfied. It was possible however, to calculate the component of $\vec{V}_{B/A}$ perpendicular to $\vec{r}$ by first calculating the component of $\vec{V}_{B/A}$ parallel to $\vec{r}$ and subtracting the resulting vector from the original $\vec{V}_{B/A}$ vector.

(2) $\hat{r} = \vec{r}/|\vec{r}|$

(3) $\vec{V}_r = (\vec{V}_{B/A} \cdot \hat{r})\, \hat{r}$

(4) $\vec{V}_p = \vec{V}_{B/A} - \vec{V}_r$

With $\vec{V}_p$ determined, equation (1) was rewritten as:

(5) $\vec{V}_p = \vec{\omega} \times \vec{r}$

Because the infinite number of $\vec{\omega}$ vectors satisfy equation (5), both the magnitude and the direction of $\vec{\omega}$ could not be uniquely determined. The angular velocity component parallel to $\vec{r}$ could not be determined due to the use of only two targets on these linkages. However, in gait analysis, the majority of rotational motion lies in the direction perpendicular to the radius and this was the primary focus of the study. Therefore, in order to solve for the magnitude of $\vec{\omega}$, the direction of $\vec{\omega}$ was chosen in the direction perpendicular to both $\vec{r}$ and $\vec{V}_p$. This axis was determined by the cross product of $\vec{r}$ and $\vec{V}_p$.

$$(6) \qquad \vec{Q} = \vec{r} \times \vec{V}_p$$

Dividing by the magnitude of $\vec{Q}$ resulted in a unit vector, $\hat{q}$, in the direction of $\vec{\omega}$:

$$(7) \qquad \hat{q} = \vec{Q} \,/\, |\vec{Q}|$$

With the direction of specified, $\vec{V}_p$, $\vec{r}$, and $\vec{\omega}$ form an orthogonal set. Rewriting equation (5):

$$(8) \qquad \vec{V}_p = |\vec{\omega}|\,|\vec{r}\,|\sin\theta \qquad \text{where } \theta = 90$$

The magnitude of $\vec{\omega}$ was easily obtained from the above expression:

$$(9) \qquad |\vec{\omega}| = |\vec{V}_p| / |\vec{r}|$$

The $\vec{\omega}$ vector was then written as the product of the magnitude, $|\vec{\omega}|$, and the unit vector, $\hat{q}$.

The angular accelerations of the upper and lower linkages were computed by methods analogous to those used to determine the corresponding angular velocities. Again, the rigid link assumption led to the following equation:

$$(10)\quad \vec{A}_B = \vec{A}_A + \vec{A}_{B/A}$$

Where $\vec{A}_A$ and $\vec{A}_B$ are the accelerations of A and B, respectively, and $\vec{A}_{B/A}$ is the acceleration of B relative to A.

The accelerations of points A and B were previously computed from the filtered data and therefore the accelerations of B relative to A could be determined.

$$(11)\quad \vec{A}_{B/A} = \vec{A}_B - \vec{A}_A$$

Unlike the case of angular velocity, $\vec{A}_{B/A}$ has both a radial and tangential component. The radial component is a result of the angular velocity while the tangential component is contributed by the angular acceleration.

$$(12)\quad \vec{A}_{B/A} = \vec{\alpha} \times \vec{r} + \vec{\omega} \times (\vec{\omega} \times \vec{r})$$

Where $\vec{\alpha}$ is the angular acceleration of the link.

From previous computations, the vectors $\vec{\omega}$ and $\vec{r}$ were known. Therefore, the quantity $\vec{\omega} \times (\vec{\omega} \times \vec{r})$ was calculated and subtracted from $\vec{A}_{B/A}$ and the resulting quantity was labeled $\vec{A}_t$.

$$(13)\quad \vec{A}_t = \vec{A}_{B/A} - \vec{\omega} \times (\vec{\omega} \times \vec{r}) = \vec{\alpha} \times \vec{r}$$

By the definition of cross product, $\vec{A}_t$ should be perpendicular to $\vec{r}$. Again, the experimental data was less than ideal due to data processing and soft tissue motion. The component of $\vec{A}_t$ perpendicular to $\vec{r}$ was found by determining the component of $\vec{A}_t$ parallel to $\vec{r}$ and subtracting the resulting vector from $\vec{A}_t$.

(14) $\vec{A}_r = (\vec{A}_t \cdot \hat{r})\, \hat{r}$

(15) $\vec{A}_p = \vec{A}_t - \vec{A}_r$

$\vec{A}_p$ is perpendicular to $\vec{r}$ and satisfies equation (13):

(16) $\vec{A}_p = \vec{\alpha} \times \vec{r}$

As with the angular velocity vector, $\vec{\alpha}$ was not uniquely defined by equation (16). For reasons analagous to those given in specifying the direction of $\vec{\omega}$, $\vec{\alpha}$ was chosen in the direction perpendicular to $\vec{r}$ and $\vec{A}_p$ in order to determine the magnitude of $\vec{\alpha}$.

(17) $\vec{r} \times \vec{A}_p = \vec{N}$

The corresponding unit vector in the direction of $\vec{\alpha}$ was defined as:

(18) $\hat{n} = \vec{N} / |\vec{N}|$

With the direction $\hat{n}$ specified, $\vec{A}_p$, $\vec{r}$ and $\vec{\alpha}$ formed an orthogonal set. Equation (16) was rewritten according to the definition of cross product:

$$(19) \quad \vec{A}_p = |\vec{\alpha}|\,|\vec{r}| \sin\theta \qquad \text{where } \theta = 90$$

The magnitude of $\vec{\alpha}$ was easily determined from the above expression:

$$(20) \quad |\vec{\alpha}| = |\vec{A}_p| / |\vec{r}|$$

The vector expression for the angular acceleration was written as the product of the magnitude of $\vec{\alpha}$ and the unit vector, $\hat{n}$.

Because the majority of leg motion during gait occurs in the plane of progression, that is, in the sagital plane, the leg was modeled as a two dimensional system of three rigid linkages (Figure 7) (3). The system was subject to the ground reaction force history recorded by the force platform. The links were connected by pins having a single axis of rotation and capable of supporting a moment. Each link was considered as a free body subject to the laws of plane Newtonian mechanics (Figures 8, 9 and 10). The point of application of the ground reaction forces, recorded by the force platform, progressed linearly from the heel to the toe in equal increments. Segment masses were obtained from the work of Wilfred T. Dempster (7). Mass moment of inertia values were obtained from Herbert M. Reynolds (17).

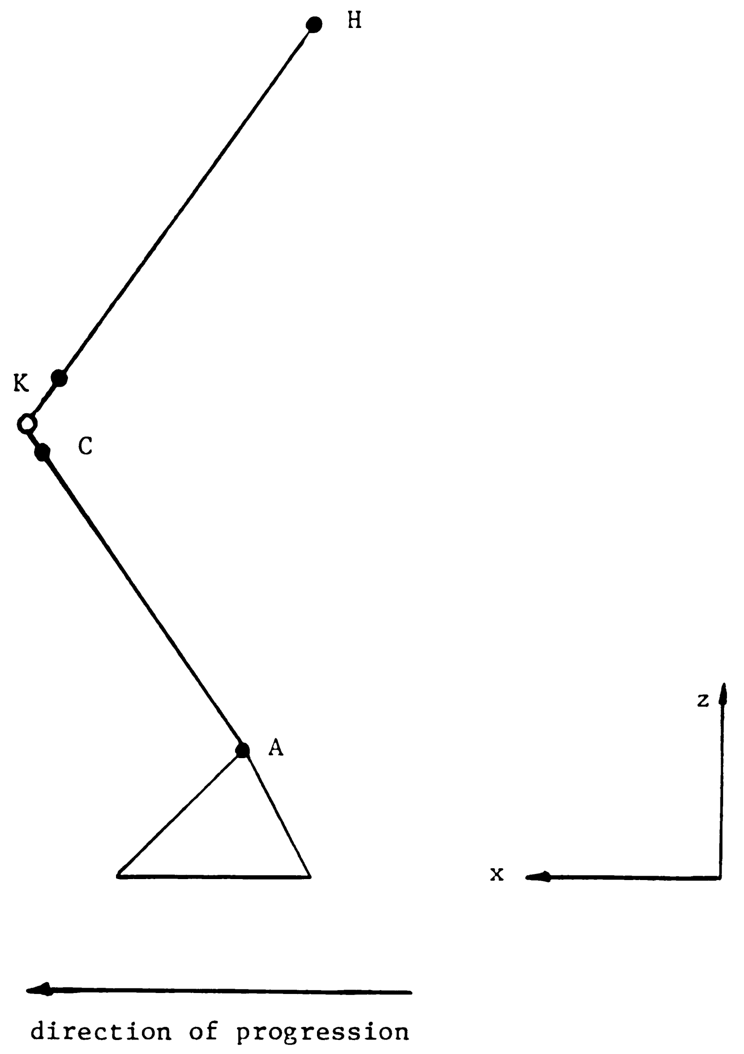

Figure 7. THREE SEGMENT RIGID LINKAGE MODEL OF THE LEG

Referring to Figure 8, the following equations were written for the rigid foot linkage:

(21) $\Sigma F_x = m_1 a_{cmx} = F_{ax} + F_{ox}$

(22) $\Sigma F_z = m_1 a_{cmz} = F_{az} + F_{oz} - m_1\vec{g}$

(23) $\Sigma M_A = I_1\vec{\alpha}_1 + (\vec{R}_{cma} \times m_1\vec{a}_a) = (\vec{R}_{cfa} \times \vec{F}_o)$
$+ \vec{M}_a + (\vec{R}_{cma} \times m_1\vec{g})$

where: m_1 = Mass of the foot

a_{cmx} = X acceleration of the CM of the foot

a_{cmz} = Z acceleration of the CM of the foot

$\vec{a}_a$ = Acceleration at the ankle

I_1 = Mass moment of inertia about the ankle

$\vec{\alpha}_1$ = Angular acceleration of the foot

$\vec{F}_o$ = Ground reaction force measured by the force platform

F_{ax} = X component of force at the ankle

F_{az} = Z component of force at the ankle

$\vec{M}_a$ = Moment at the ankle

Equations (21), (22) and (23) contain the unknowns F_{ax}, F_{az}, a_{cmx}, a_{cmz}, and $\vec{M}_a$. In order to solve for F_{ax}, F_{az} and $\vec{M}_a$, the acceleration of the center of mass of the foot was determined by applying the rigid link theory to the foot and utilizing the known acceleration of the ankle and the angular velocity and angular acceleration of the foot.

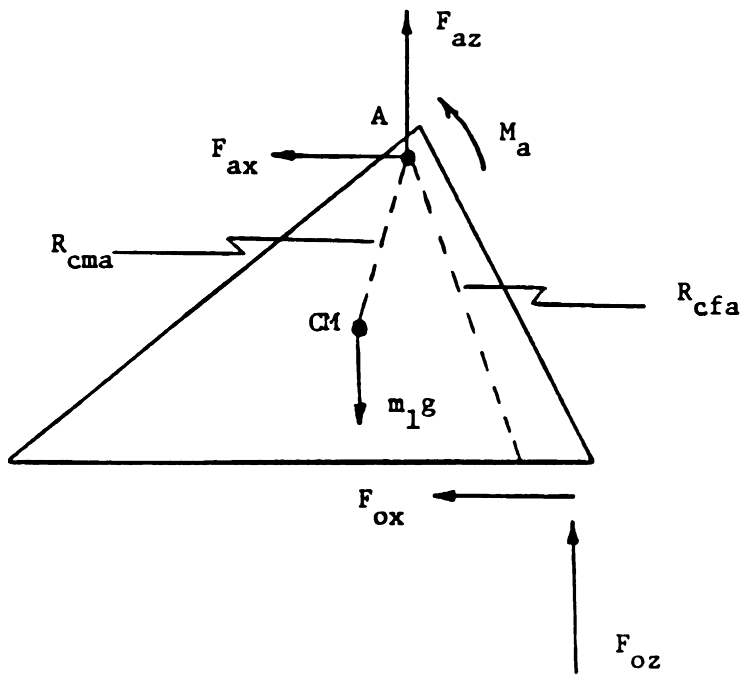

Figure 8. FREE BODY DIAGRAM OF THE FOOT

(24) $\vec{A}_a = \vec{A}_{cm} + \vec{A}_{a/cm}$

Rearranging equation (24):

(25) $\vec{A}_{cm} = \vec{A}_a - \vec{A}_{a/cm}$

The relative acceleration, $\vec{A}_{a/cm}$, is composed of a radial and a tangential component resulting from the angular velocity and angular acceleration of the foot.

(26) $\vec{A}_{a/cm} = \vec{\alpha}_f \times \vec{R}_{cma} + \vec{\omega}_f \times (\vec{\omega}_f \times \vec{R}_{cma})$

Substituting equation (26) into (25):

(27) $\vec{A}_{cm} = \vec{A}_a - (\vec{\alpha}_f \times \vec{R}_{cma}) + \vec{\omega}_f \times (\vec{\omega}_f \times \vec{R}_{cma})$

The x and z components of equation (27) were substituted into equations (21), (22) and (23) to yield the ankle reaction forces, F_{ax} and F_{az} and the moment at the ankle, $\vec{M}_a$.

Referring the Figure 9, the folowing equations were written for the lower leg rigid link:

(28) $\Sigma F_x = m_2 a_{cmx} = -F_{ax} + F_{kx}$

(29) $\Sigma F_z = m_2 a_{cmz} = -F_{az} + F_{kz} - m_2\vec{g}$

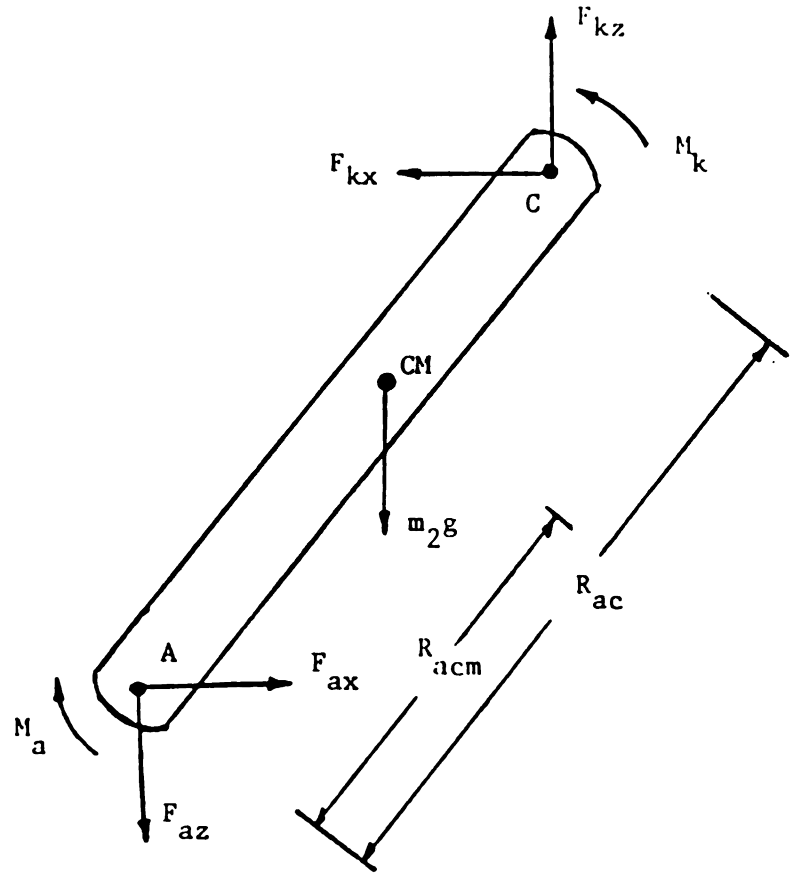

Figure 9. FREE BODY DIAGRAM OF THE LOWER LEG SEGMENT

$$(30) \quad \Sigma M_a = I_2\vec{\alpha}_2 + (\vec{R}_{acm} \times m_2\vec{a}_a) = (\vec{R}_{ac} \times \vec{F}_k) + \vec{M}_k + (\vec{R}_{acm} \times m_2\vec{g}) - \vec{M}_a$$

where: m_2 = Mass of the lower leg segment

a_{cmx} = X acceleration of the CM of the lower leg

a_{cmz} = Z acceleration of the CM of the lower leg

$\vec{a}_a$ = Acceleration at the ankle

I_2 = Mass moment of inertia of the lower leg

$\vec{\alpha}_2$ = Angular acceleration of the lower leg

F_{kx} = X component of force at the knee

F_{kz} = Z component of force at the knee

$\vec{M}_k$ = Moment at the knee

Equations (28), (29) and (30) contain the unknowns F_{kx}, F_{kz}, $\vec{M}_k$. a_{cmx} and a_{cmz}. a_{cmx} and a_{cmz} were easily solved for using the method outlined in the rigid linkage section of this chapter. The knee reaction forces, F_{kx} and F_{kz}, and the knee moment $\vec{M}_k$, were then determined directly from the above equations.

The free body diagram for the upper leg segment is presented in Figure 10. The following equations were written for the upper leg rigid linkage:

$$(31) \quad \Sigma F_x = m_3 a_{cmx} = -F_{kx} + F_{hx}$$

$$(32) \quad \Sigma F_z = m_3 a_{cmz} = -F_{kz} + F_{hz} - m_3\vec{g}$$

$$(33) \quad \Sigma M_k = I_3\vec{\alpha}_3 + (\vec{R}_{kcm} \times m_3\vec{a}_k = (\vec{R}_{kh} \times \vec{F}_h) + \vec{M}_h + (\vec{R}_{kcm} \times m_3\vec{g}) - \vec{M}_k$$

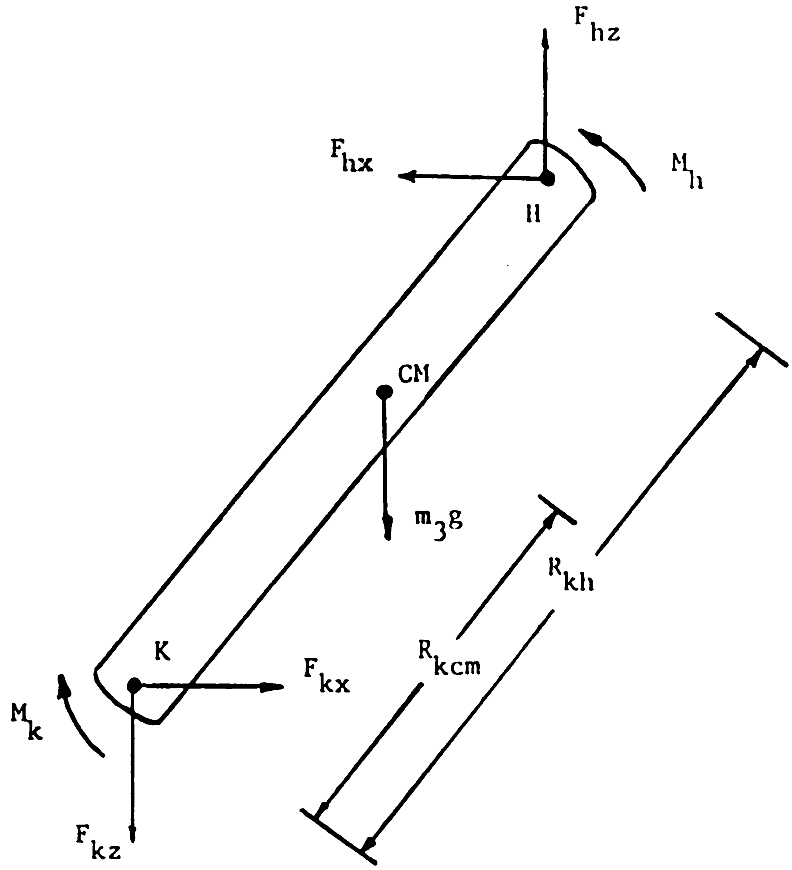

Figure 10. FREE BODY DIAGRAM OF THE UPPER LEG SEGMENT

where: m_3 = Mass of the upper leg segment

a_{cmx} = X acceleration of CM of the upper leg

a_{cmz} = Z acceleration of CM of the upper leg

$\vec{a}_k$ = Acceleration at the knee

I_3 = Mass moment of inertia of the upper leg

$\vec{\alpha}_3$ = Angular acceleration of the upper leg

F_{hx} = X component of force at the hip

F_{hz} = Z component of force at the hip

$\vec{M}_h$ = Moment at the hip

Again, utilizing the method to determine a_{cmx} and a_{cmz}, the unknowns F_{hx}, F_{hz}, and $\vec{M}_h$ were easily solved from equations (31), (32) and (33).

V. RESULTS AND DISCUSSION

The results of the experimental data collection, angular velocity determination and calculation of the external joint forces and moments are presented in the following section. Each of the graphs represents stance phase of gait for the left leg. Time zero corresponds to foot strike, and the end of the plot corresponds to toe off. All data, with the exception of the ground reaction force plots, are presented after filtering.

An example of the ground reaction curves measured by the force platform is shown in Figures 11 and 12. These curves represent the forces exerted on the ground by the body and follow the force platform sign convention shown in Figure 13. Therefore, the ground exerts a force on the body equal in magnitude and opposite in direction to the ground reaction force. The total contact time was 184 milliseconds. The vertical force component, (FZO), of the ground reaction force exhibits a double peaked curve, the first peak rising to a value of approximately 1300 Newtons (2.25 times body weight) in 15 milliseconds. The second peak attains a maximum value of 1700 Newtons (2.94 BW) 63 milliseconds after initial contact. The anterior-posterior force component (FXO) displays a slight positive peak of 60 Newtons (.10 BW), directed opposite of the direction of progression, which decreases to zero after 10 milliseconds. The force falls to a negative peak of 237 Newtons (0.41 BW) in 39 milliseconds. The curve then rises to a positive peak value, nearly equal in magnitude to the first peak, 130

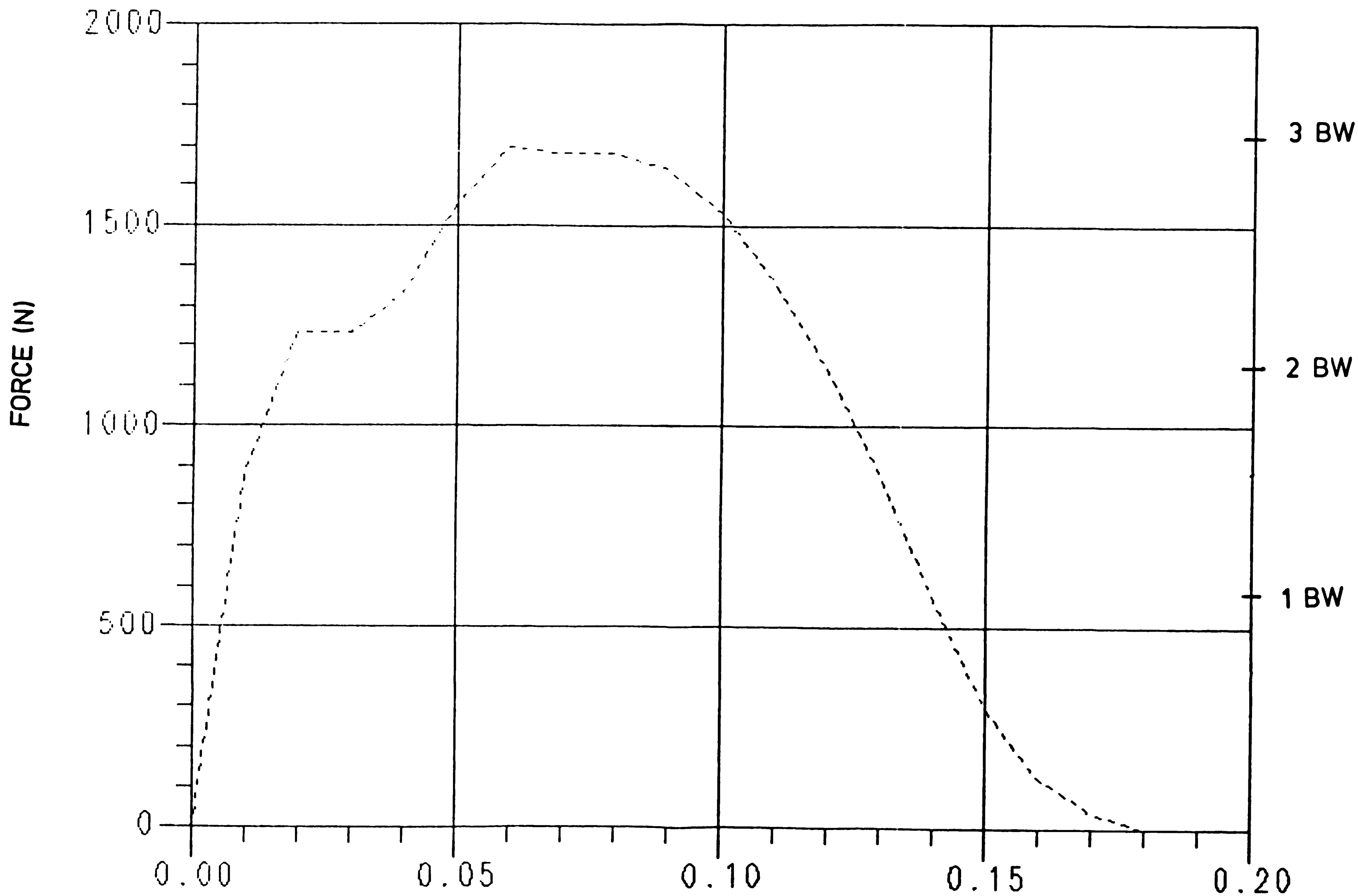

Figure 11. VERTICAL GROUND REACTION FORCES

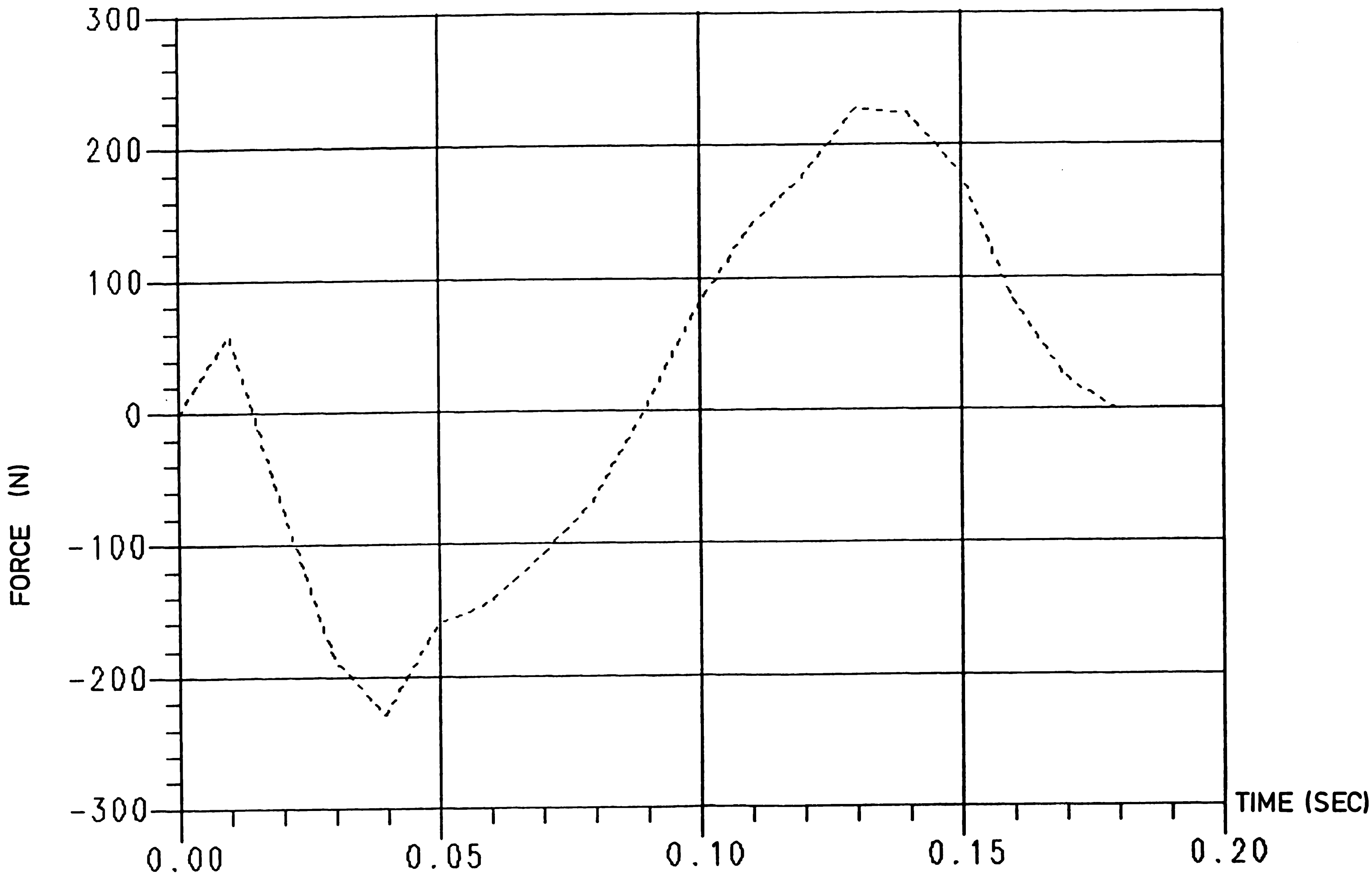

Figure 12. ANTERIOR/POSTERIOR GROUND REACTION FORCES

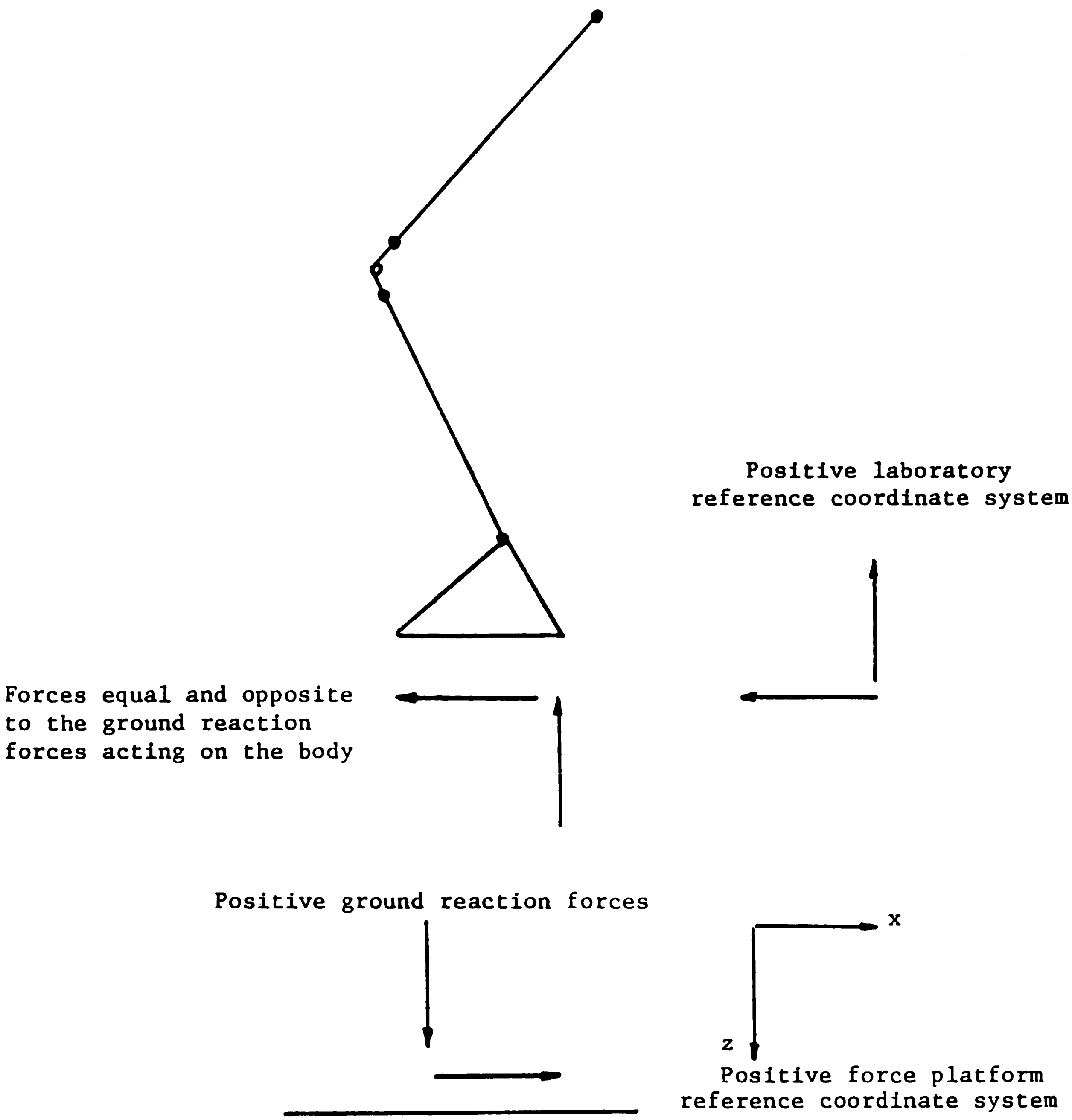

Figure 13. POSITIVE ACTION AND REACTION FORCES
AT THE GROUND/FOOT INTERFACE

milliseconds after foot strike. The transition from braking to propulsion occurs at approximately 48% of the total contact time. The medial-lateral force component is very small in comparison to the vertical and anterior-posterior components and was not considered for the two dimensional analysis. All components showed excellent comparison in both magnitudes and occurence times with the data published by Cavanagh and Lafortune (5).

Figure 14 and 15 display typical angular velocity curves for the left ankle and knee joints during stance phase. These plots show the difference between the angular velocities of the segments above and below the joint. Following foot contact, the ankle joint curve shows an increase in rate of dorsiflexion with a peak value of 8 radians per second, 70 milliseconds after initial contact. The ankle is rapidly dorsi-flexing to halt the downward vertical velocity of the body. At the onset of the propulsion stage, the rate of dorsiflexion quickly decreases, changing to plantarflexional angular velocity 30 milliseconds into propulsion. This rapid change from dorsiflexion to plantarflexion is necessary to successfully propel the body forward and upward. The rate of plantarflexion increases to a value of 12 radians per second, 145 milliseconds after initial contact. The magnitude decreases as toe off approaches, attaining a final value of 7 radians per second.

The angular velocity curve for the knee (Figure 15) begins with an increase in the rate of flexion, rapidly peaking 30 milliseconds after foot strike with a value of 5.5 radians per second. The rate of flexion begins decreasing, becoming zero at approximately the same time the transition from braking to propulsion occurs. In other words, the knee is flexed for the duration of the braking phase; first rapidly flexing

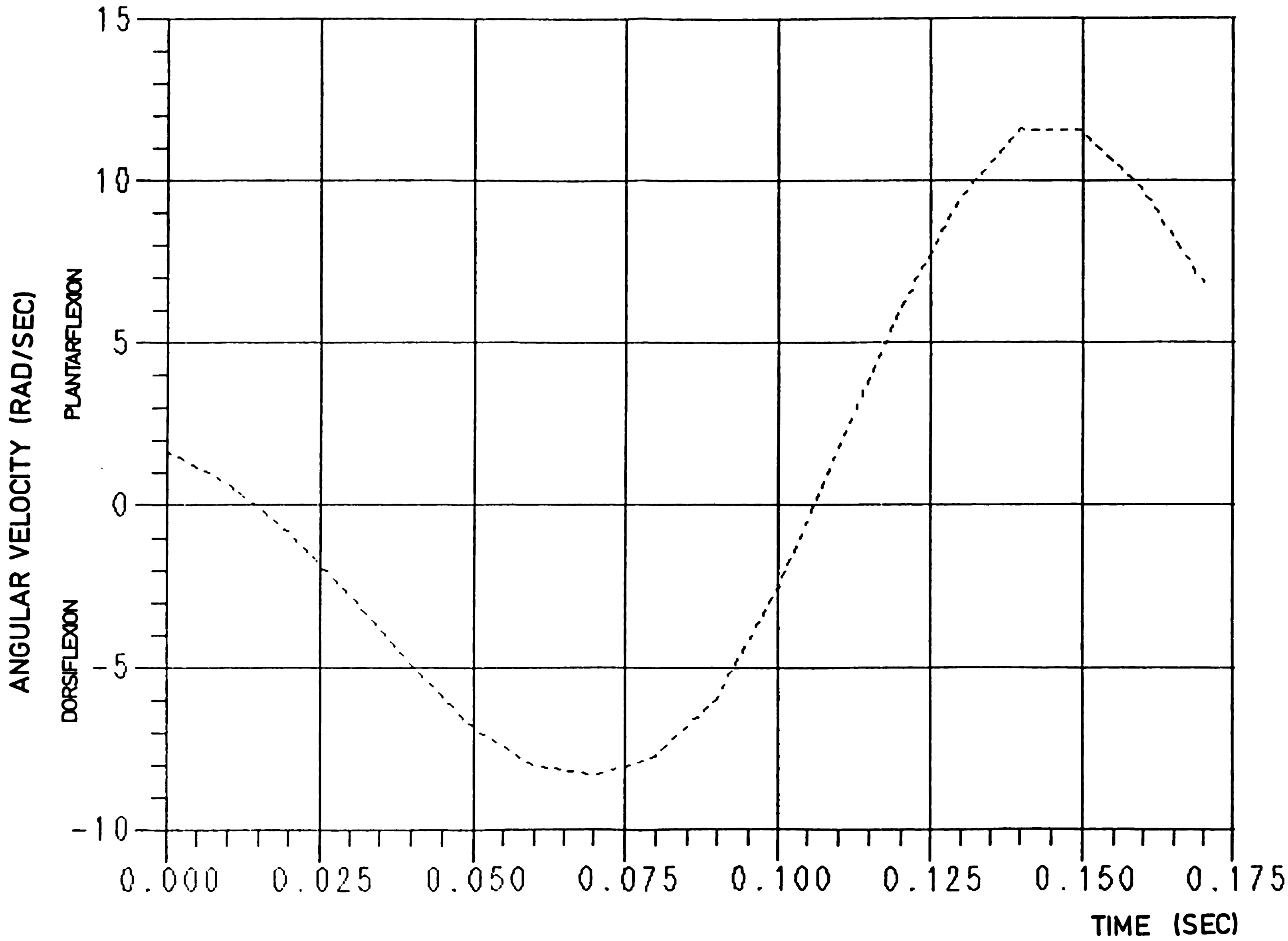

Figure 14. RELATIVE ANGULAR VELOCITY AT THE ANKLE

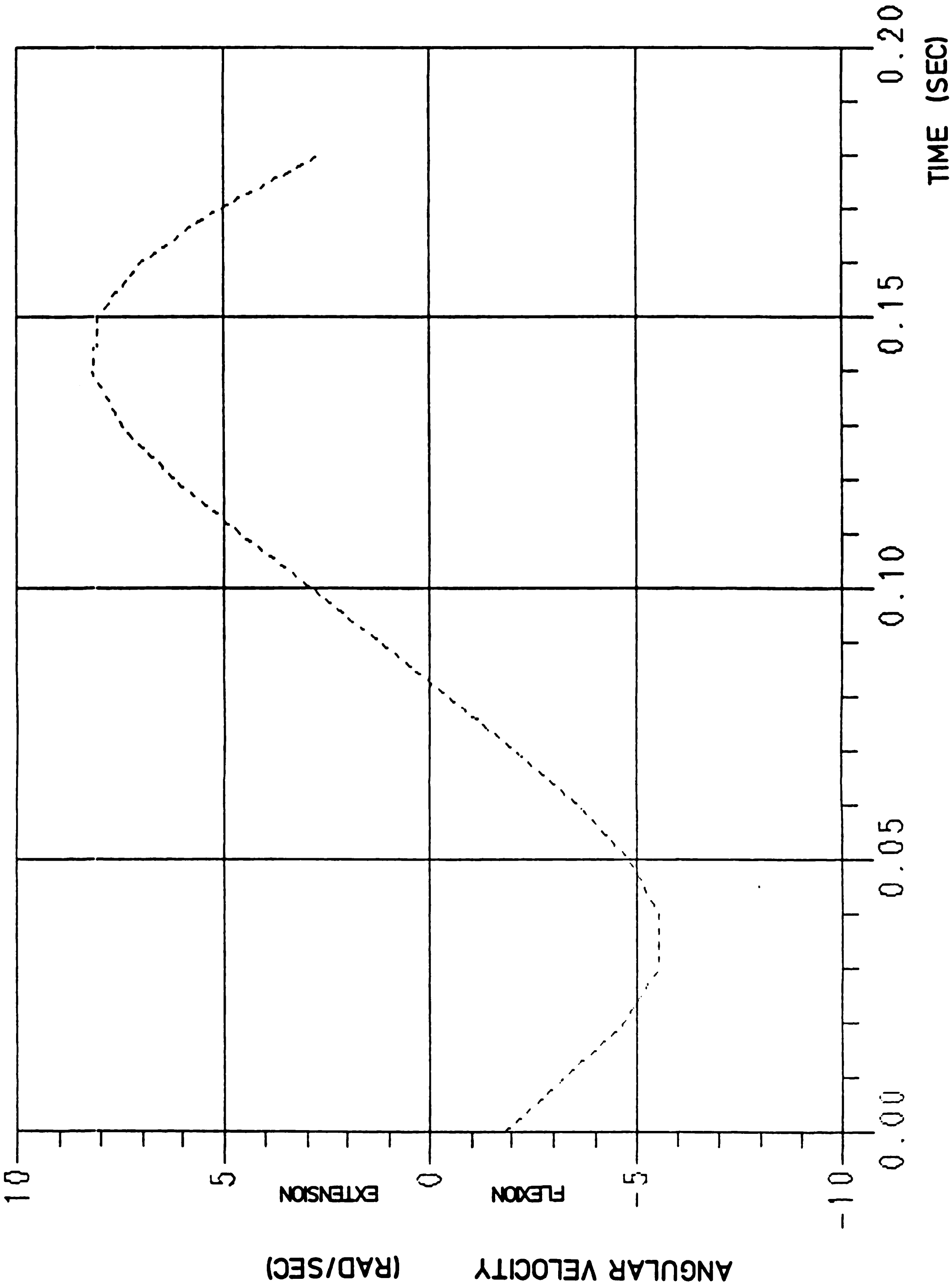

Figure 15. RELATIVE ANGULAR VELOCITY AT THE KNEE

to hinder the downward velocity of the body then slowing down in preparation for propulsion phase. Entering propulsion, the extensional angular velocity increases to a peak value of 8 radians per second 140 milliseconds into contact phase. As toe off approaches, the rate of extension decreases to a final value of 2.5 radians per second. The knee joint extends in an effort to propel the body forward. Both curves show good comparison in amplitudes and tendencies with those published by Ito, et al (11).

Forces in the sagittal plane at the ankle, knee and hip are shown in Figures 17 and 19. These plots represent the joint reaction forces at the proximal end of each segment due to the forces exerted by the segment below it, with a sign convention consistant with the laboratory reference coordinate system (Figure 16). In the case of the ankle joint, the forces are exerted on the foot segment by the ground. The vertical force curves (Figure 17) all display a pattern similar to the vertical ground reaction curve -- an initial peak approximately 2.2 times body weight followed by a second peak 2.9 times body weight. The first peak occurs 20 milliseconds after foot strike and is the reaction to the initial impact. The joint compressive forces rise from the first peak to the second, 60 milliseconds into ground contact. The curves remain somewhat constant as the body rolls across the supporting leg and eventually decrease at toe off to approximately 0.2 times body weight. At this time, the maximum vertical force occurs at the ankle. while the forces at the knee and hip are attenuated by the gravitational and vertical acceleration effects on the shank and thigh (Figure 18).

The anterior-posterior forces, (Figure 19), show similar tendencies for the ankle and knee joints, while the hip response is markedly

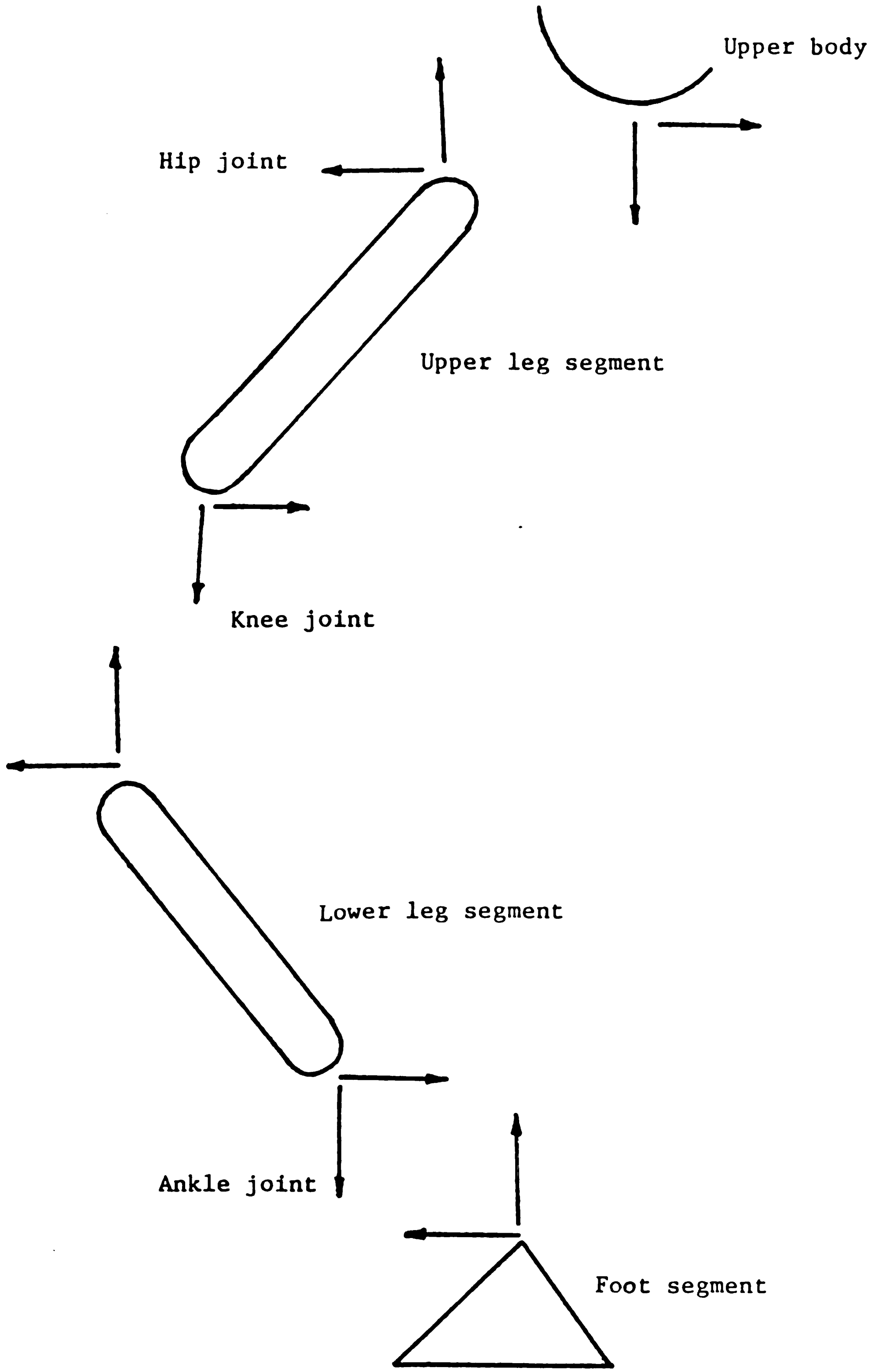

Figure 16. POSITIVE SIGN CONVENTION FOR THE EXTERNAL JOINT FORCES

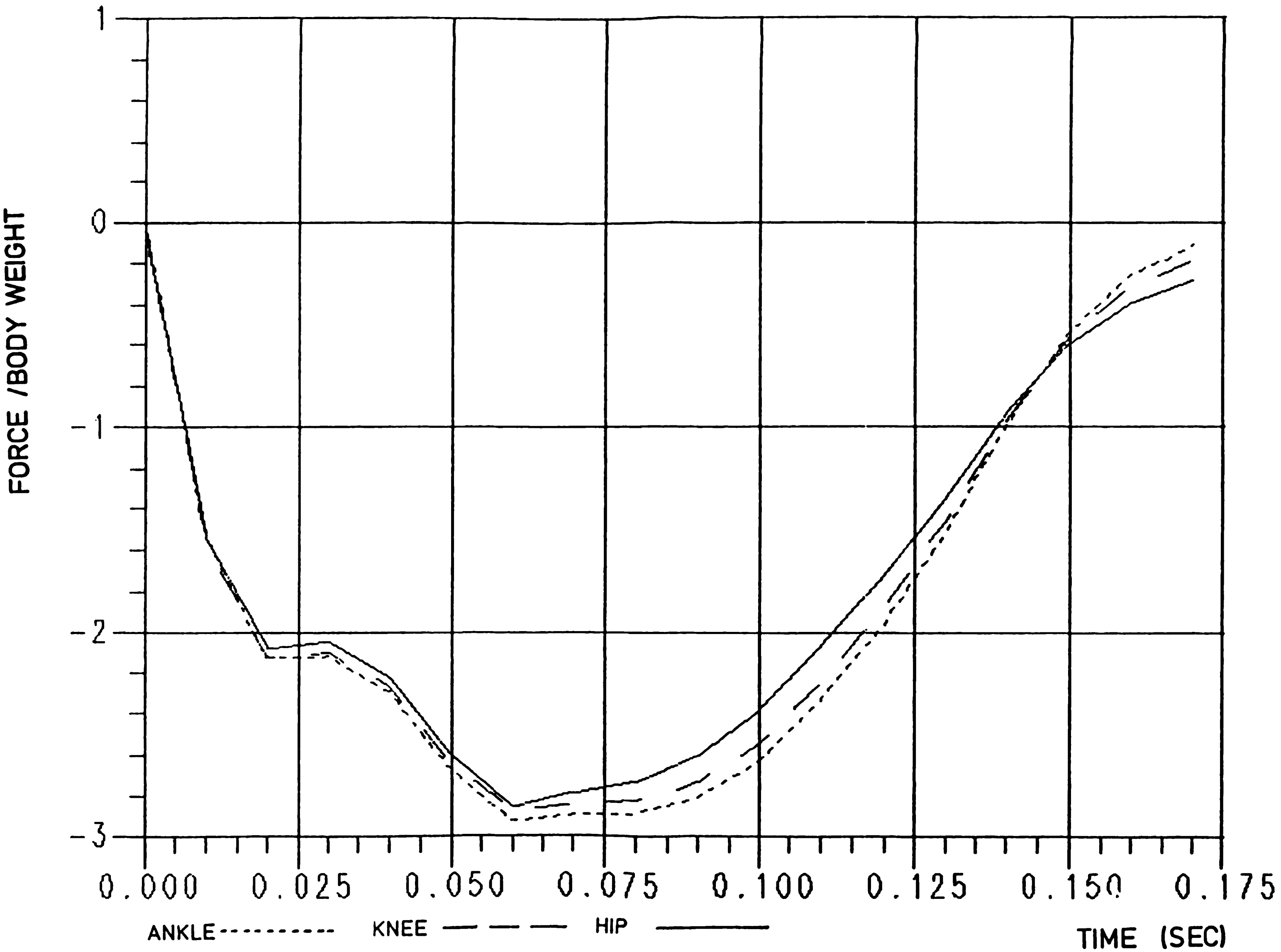

Figure 17. VERTICAL FORCES AT THE ANKLE, KNEE AND HIP

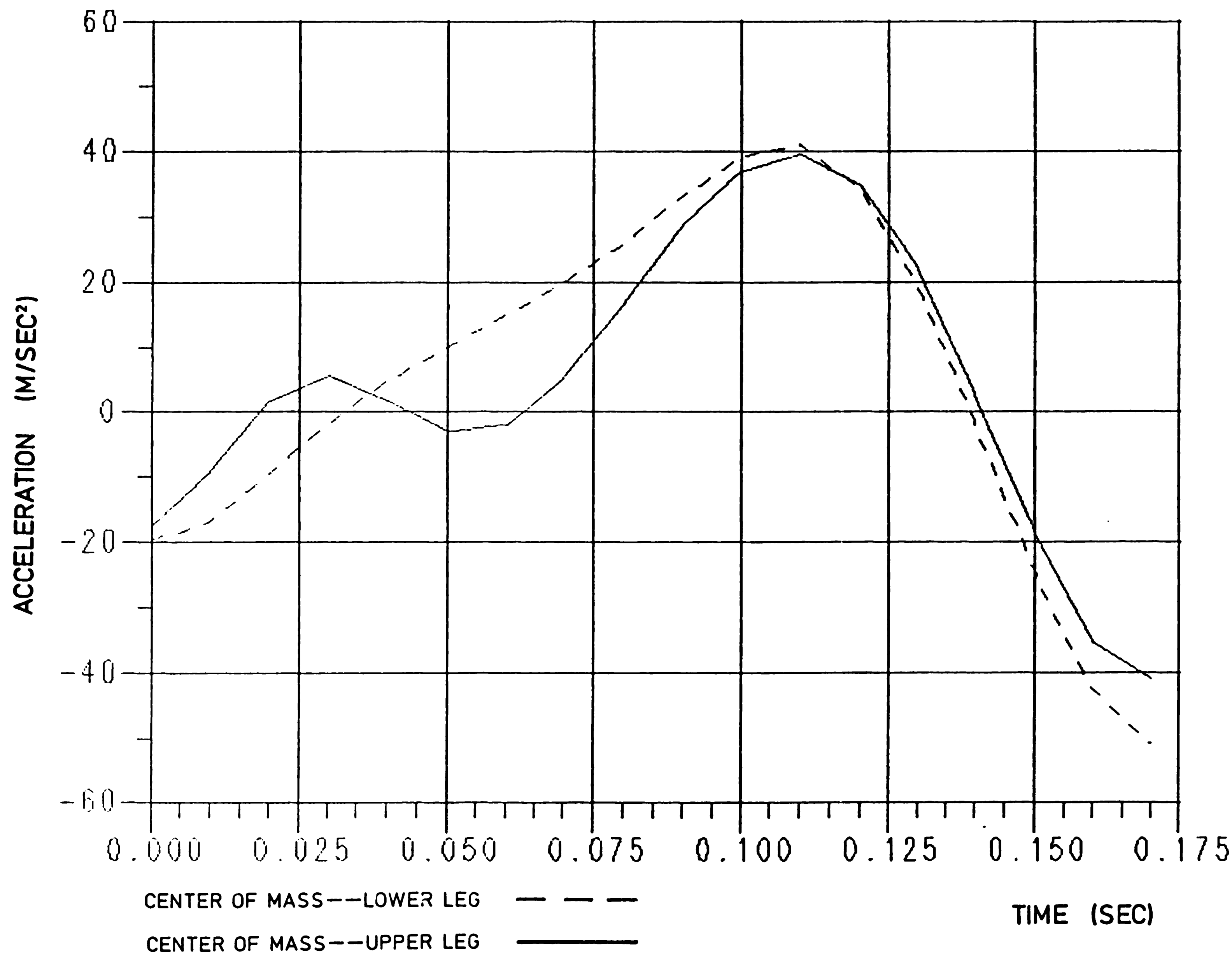

Figure 18. VERTICAL ACCELERATIONS OF THE CENTER OF MASS FOR THE UPPER AND LOWER LINKAGES

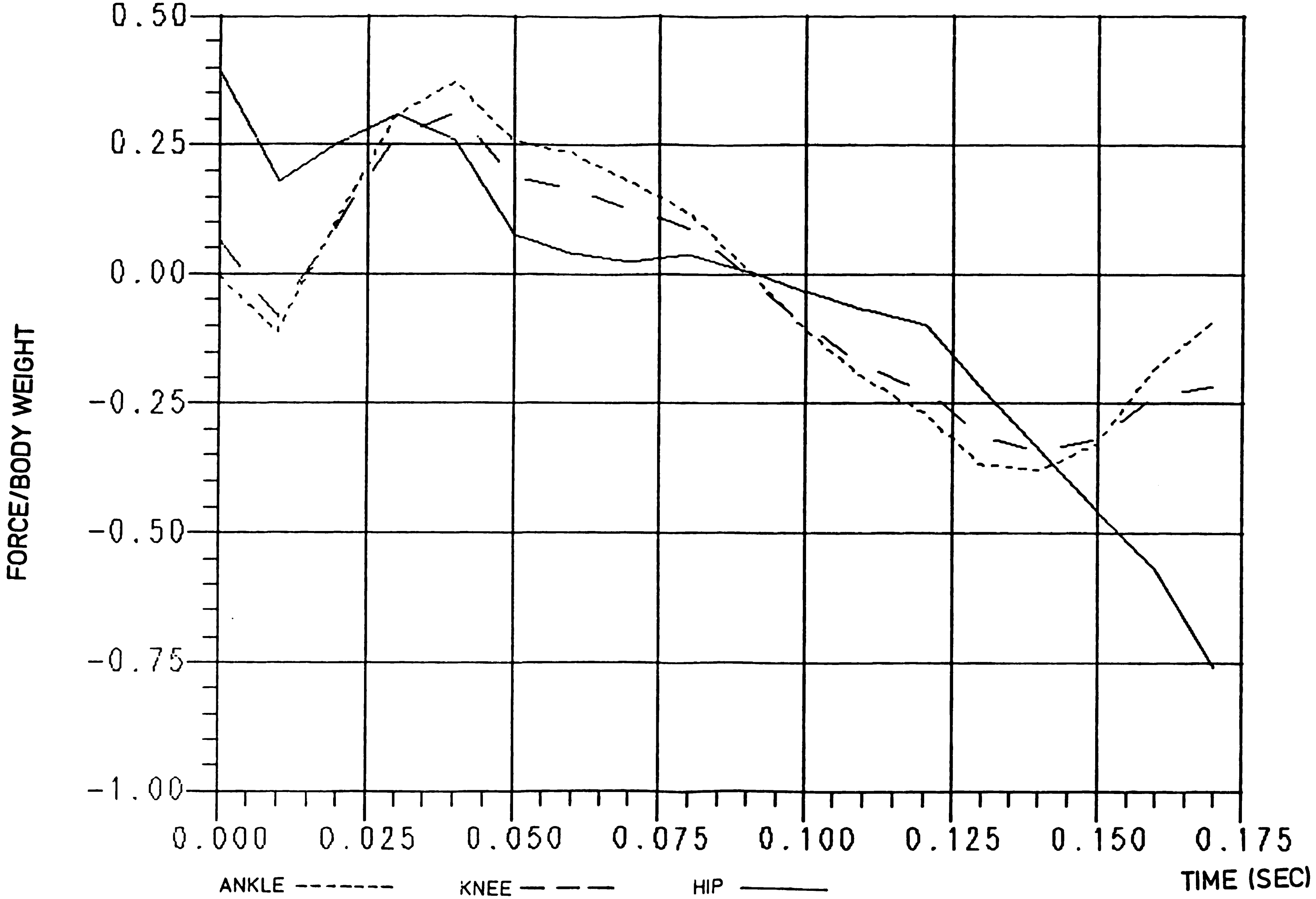

Figure 19. ANTERIOR/POSTERIOR FORCES AT THE ANKLE, KNEE AND HIP

different. The ankle and the knee display a slight negative dip of 0.10 times body weight immediately after heel strike, indicating the segments above the joint experience a force in the anterior direction while those below the joint experience a posteriorly directed force (Figure 16). As the ground force on the body becomes posterior, the force curves become positive, with the ankle force reaching a value of 0.35 times body weight and the knee force attaining a value of 0.30 times body weight. Therefore, during braking, the ground exerts a force in the posterior direction on the foot, and the ankle joint reacts with an anterior force on the foot segment and a posterior force on the lower leg segment. At the knee joint, the lower leg experiences an anterior force while the upper leg reacts with a posterior force. The peak forces of the ankle and knee joints are attenuated in comparison with the corresponding ground reaction forces due, in part, to the posterior acceleration of the calf and thigh masses (Figure 20). Both joint forces decrease in magnitude and change direction at the time of transition from braking to propulsion. The peak negative forces occur approximately 135 milliseconds after initial contact, with the ankle force attaining a value of 0.35 times body weight and the knee force reaching a value of 0.37 times body weight. During propulsion, the foot pushes off the ground, exerting a force in the posterior direction, and therefore, the ground input force on the foot is in the anterior direction. The reaction at the ankle joint is posterior at the foot segment and anterior at the lower leg segment. The knee joint experiences a posterior force at the lower leg segment and an anterior force at the upper leg segment. The accelerations of the calf and thigh masses during this phase are directed anteriorly. At the approach of

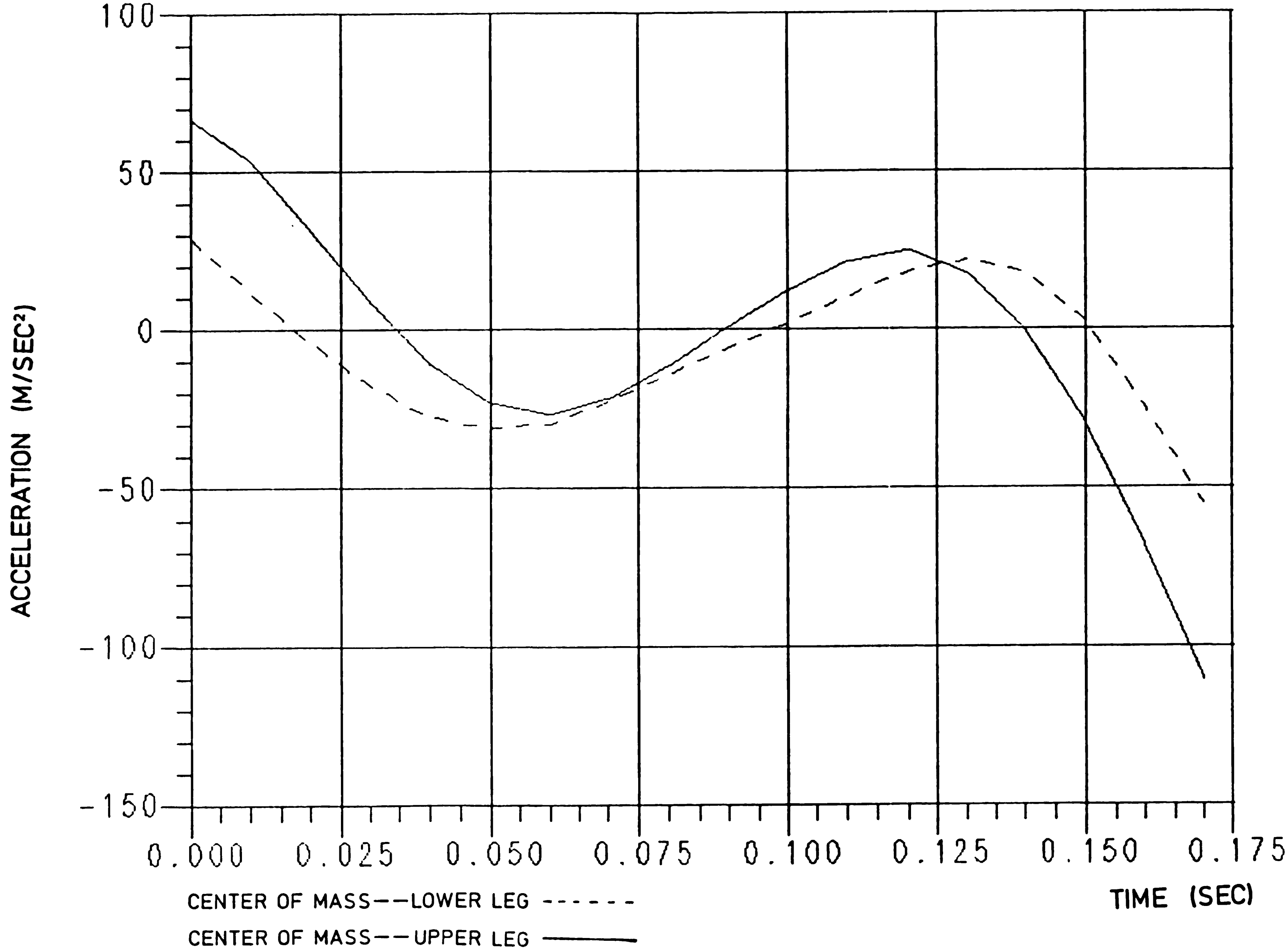

Figure 20. ANTERIOR/POSTERIOR ACCELERATIONS OF THE CENTER OF MASS FOR THE UPPER AND LOWER LINKAGES

toe off, the ankle force decreases to 0.10 times body weight, while the knee force decreases to 0.21 times body weight. The ankle and knee forces do not return to zero at toe off due to the increasingly negative accelerations acting posteriorly on the calf and thigh masses.

The horizontal force at the hip has an initial positive value of 0.4 times body weight directed anteriorly on the upper leg segment and posteriorly on the torso. The hip force during early braking is larger than the forces calculated at the ankle and knee in order to decelerate the relatively large mass of the upper body. The force rapidly decreases to a magnitude of approximately 0.04 times body weight, 60 milliseconds after heel strike. It remains relatively constant for 20 milliseconds, then decreases to zero at the onset of propulsion stage. During propulsion, the hip force becomes negative, indicating that the force on the upper leg segment is now directed posteriorly while the force on the upper body is directed anteriorly. In the first 30 milliseconds of propulsion, the force gradually increases to a value of 0.1 times body weight, followed by a rapid increase to a final value of 0.75 times body weight. Therefore, the upper body is thrust forward and upward into swing phase during the latter portion of propulsion phase.

The moments of the ankle, knee and hip are presented in Figure 21. The labels "flexor" and "extensor" in Figure 19 refer to the ankle and hip curves only. A "flexor" moment at the knee joint is a positive moment while an "extensor" moment at the knee joint is a negative moment. These plots indicate the muscle groups that are dominate during stance phase. Due to the nature of the study, individual muscle contributions cannot be determined.

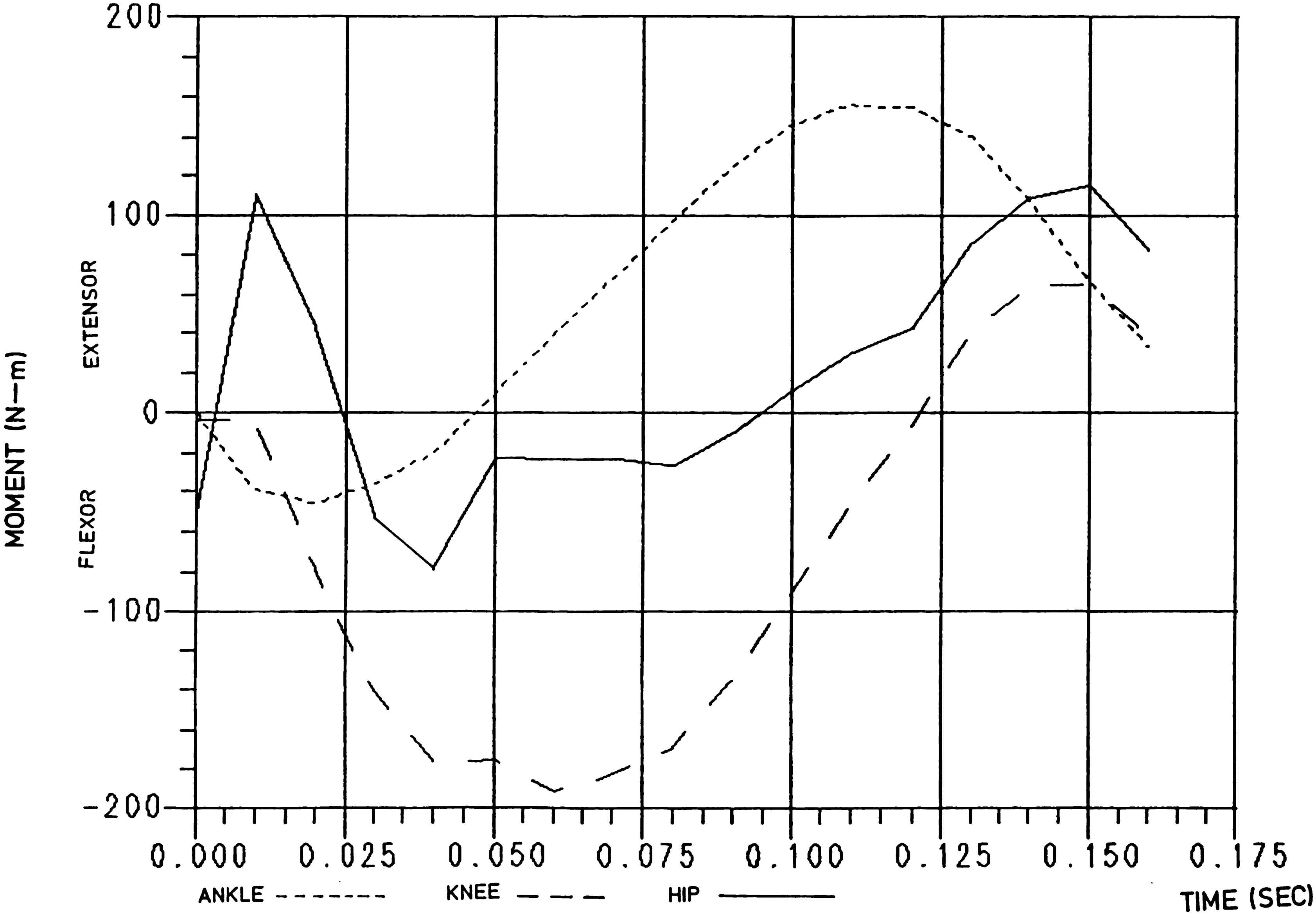

Figure 21. MOMENTS AT THE ANKLE, KNEE AND HIP JOINTS

As the foot contacts the ground, the ankle immediately brakes to terminate the rapid downward vertical velocity of the body. This is accomplished by an initial dorsiflexor moment with a maximum value of 45 Newton-meters. Approximately halfway into the braking phase, the plantarflexors achieve dominance, lowering the foot to the ground. The plantarflexor moment peaks 30 milliseconds into propulsion phase with a value of 160 Newton-meters. This moment generates the forward and upward velocity necessary to propel the body into swing phase. As toe off approaches, the plantarflexor moment decreases to zero to position the leg and foot for swing phase.

At foot strike, the knee responds to the impact with a slight extensor moment of approximately 8 Newton-meters. As knee extensors are rapidly employed to halt the downward velocity of the body, a peak extensor moment of 190 Newton-meters is generated 60 milliseconds after foot strike. With braking completed, the extensor moment decreases to project the body forward and upward. The moment returns to a zero value 120 milliseconds into stance phase and changes to a flexor moment late in propulsion phase. The flexor moment peaks at a value of 60 Newton-meters and decreases to 15 Newtom-meters as the foot leaves the ground.

The hip extensors rapidly attain a peak value of 115 Newton-meters, 10 milliseconds after foot strike. This extensor moment continues to aid in braking the body for an additional 15 milliseconds. The hip then experiences a flexor moment which continues for the duration and peaks at a value of 80 Newton-meters of braking phase. The purpose of the flexor moment is to slow the downward acceleration of the body after the forefoot is lowered to the ground. Late in braking phase the moment decreases in magnitude, enabling the trunk to roll over the supporting leg. The hip moment changes direction early in propulsion phase. The extensor moment peaks at a value of 110 Newton-meters and generates the necessary acceleration to propel the body forward and upward into the swing phase. The rapid change in the hip moment during the interval of 40 to 80 milliseconds after foot strike may possibly by attributed to soft tissue motion or the linear progression of the ground reaction forces.

The ankle and knee moment curves compared favorably with the published results fo Mann (12) and Winter (22, 23). The peak magnitudes of the ankle and knee moments were higher than those published by Winter (22) and lower than those published by Mann (12). While this can partially be attributed to differences in subject mass and body build, it also is an expected result as the former study analyzed slow jogging while the later study investigated sprinting. In comparing the hip moment curves from the three previous studies and the current investigation, it is observed that a clearly defined moment pattern does not exist. The extensor/flexor/extensor tendency recorded in this investigation was not seen in any of the three running papers, and among the three publications, a recurrent tendency was not established. It was for this reason that Winter defined the support moment—the algebraic sum of the extensor moments at the three joints (22). The support moment was calculated for this study and is presented in Figure 22. The theory of overall limb support states the support moment displays a net extension for the duration of stance phase and the results from this study support this theory.

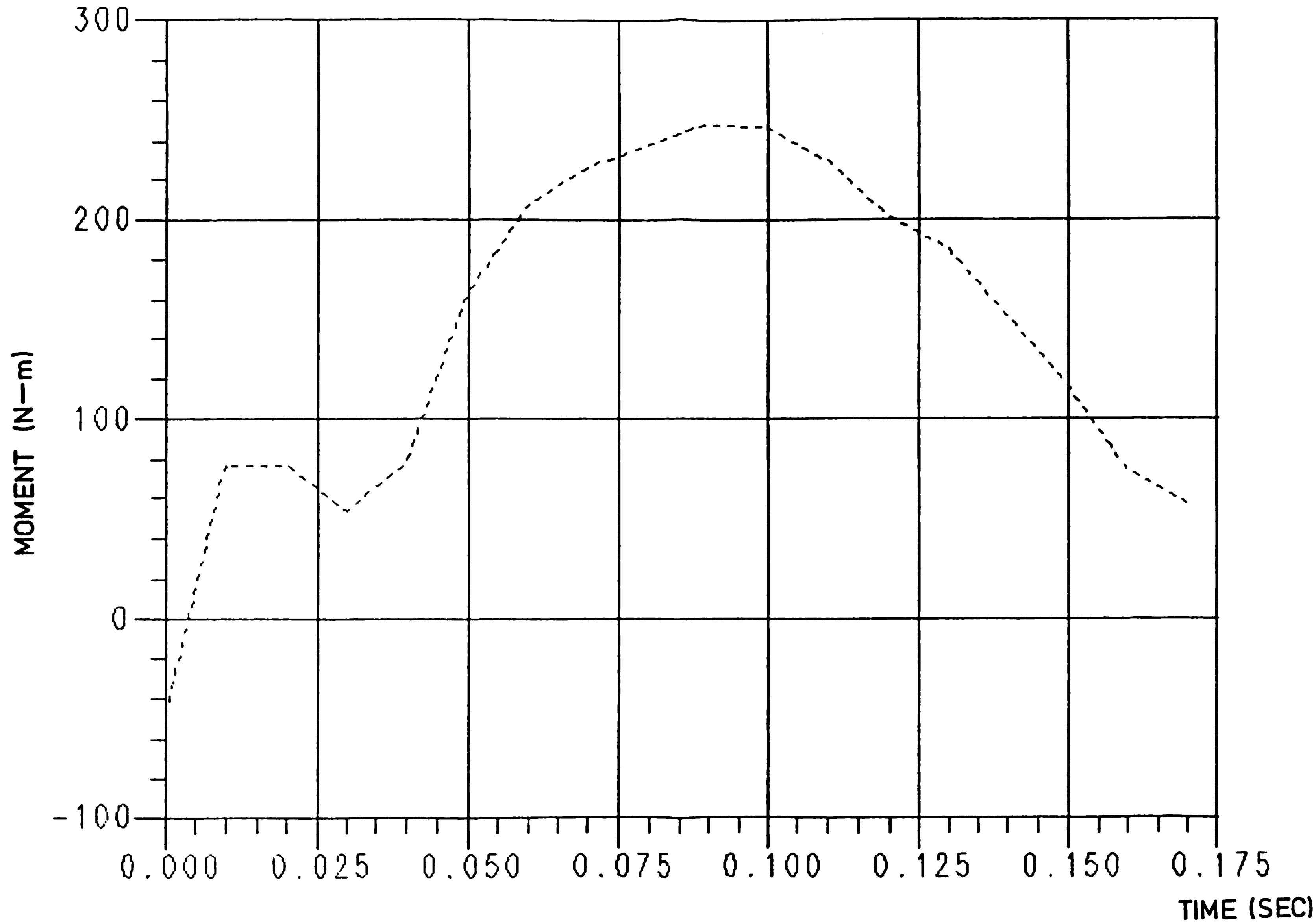

Figure 22. SUPPORT MOMENT OF THE LOWER LIMB

VI. CONCLUSION

The main purpose of this research was to develop a procedure for the computation of the dynamic parameters used in the description of human locomotion. The specific form of locomotion analyzed in this study was running. While a great deal of information is available regarding the dynamics of walking, very little research has been conducted on the dynamics of running. With the exponential increase in the number of people participating in this activity, the need for research in this area is clearly justified.

The experimental set up included two high speed cine cameras in stereo configuration to obtain the position data of the limb segments. The velocities and accelerations were calculated from the three dimensional position data, and in turn, were used to compute the angular velocity and acceleration components perpendicular to the radius and velocity vectors. The assumption that the angular velocity vector is perpendicular to the linkage axis and relative velocity vectors produced results that compared very well with those published by Ito, et al (11). At this point in the analysis, a two dimensional approach was taken because it was considerably less complex than a three dimensional analysis, and the forces and moments of greatest importance in limb stability are still obtained. Because the filming incorporates all three dimensions, a three dimensional analysis is possible with the use of more targets and the additional dynamic equations.

The results from this study indicate the maximum vertical forces at the ankle, knee and hip joints approach a value of three times body weight. The vertical force is directed downward on the segment inferior to the joint and upward on the segment superior to the joint for the duration of stance phase. The horizontal forces at the three joints all display a positive force for the duration of braking phase -- an anterior force on the segment inferior to the joint and a posterior force on the segment superior to the joint. During propulsion, the three forces are negative, indicating a posterior force on the segment inferior to the joint and an anterior force on the segment superior to the joint. The difference in the forces at the proximal and distal end of any segment can be correlated directly to the acceleration curve in the same direction.

The moments in this investigation indicate that at the onset of braking phase, the hip joint moment experiences an extensor moment nearly three times as large as the extensor moment at the knee joint and the dorsiflexor moment at the ankle joint. This large hip moment is necessary to decelerate the upper body during the braking phase. In addition, the moment at the hip joint is responsible for the majority of lower limb support during early braking phase. During midstance, the knee experiences the greatest peak moment exceeding the ankle extensor moment by 150 Newtom-meters and the hip flexor moment by 175 Newtom-meters and is the greatest contributor to lower limb support. The body is thrust forward and upward during early propulsion by extensor moments at the ankle and knee joints. Final propulsion into swing phase is accomplished by an extensor moment at the hip joint. Lower limb support during braking is accomplished by contributions from both the ankle and the hip extensor moments.

Determining the kinetic parameters during the stance phase of running is a contribution to the biomechanical investigation of gait. Knowledge of these variables is essential in determining the mechanical power, energy transfer and internal joint forces of the limb segments. The devised research protocol can be used to record baseline force and moment data for comparisons in running speed, running style and athletic footwear. Medical applications also exist to evaluate the modality of different therapeutic methods, rehabilitation procedures and prosthetic design.

BIBLIOGRAPHY

BIBLIOGRAPHY

1. Beavis, G.C. (1985). Personal correspondence.

2. Braune, W. and Fischer, O. (1872). uber den Schwerpunkt des menschlichen Forpers mit Ruecksicht auf die Aursruestung des deutschen Infanteriesten (Concerning the Center of Gravity of the Human Body with Reference to the Equipment of the German Infantrymen), Abhandlungen der Koenigl. Saechs. Gesellschaft der Wissenschaft, Vol. 15.

3. Bresler, E. and Frankel, J.B. (1950). The Forces and Moments in the Leg During Walking, J. Appl. Mech., **72**, 27-36.

4. Cavanagh, P.R. (1981). The Running Shoe Book, Mountain View, CA: World Publications, 1-95.

5. Cavanagh, P.R. and Lafortune, M.A. (1980). Ground Reaction Forces in Distance Running, J. Biomechanics, **13**, 397-401.

6. Crowninshield, R.D., Johnston, R.C., Andrews, J.G. and Brand, R.A. (1978). A Biomechanical Investigation of the Human Hip, J. Biomechanics, **11**, 75-85.

7. Dempster, W.T. Space requirements of the seated operator. In: WADC Technical Report 55-159. Wright-Patterson Air Force Base, Ohio, 1955.

8. Elftman, H. (1939). Forces and Energy Changes in the Leg During Walking, Am. J. Physiol., **125**, 339-356.

9. Gilbert, J.A., Maxwell, G.M., McElhaney, J.H. and Clippinger, F.W. (1984). A System to Measure the Forces and Moments at the Knee and Hip During Level Walking, J. of Orthopaedic Research, **2**, 281-288.

10. Grood, E.S. and Suntay, W.J. (1983). A Joint Coordinate System for the Clinical Description of Three Dimensional Motions: Applications to the Knee, J. of Biomechanical Eng., **105**, 136-144.

11. Ito, A., Komi, P.V., Sjodin, C., Bosco, C. and Karlsson, J. (1983). Mechanical Efficiency of Positive Work in Running at Different Speeds. Med. Sci. Sports., **15**, 299-308.

12. Mann, R.V. (1981). A Kinetic Analysis of Sprinting, Medicine and Science in Sports and Exercise, **13**, 5, 325-328.

13. Marey, E.J. and G. Masson (1885). La methode graphique dans les sciences experimentales (The Graphic Method in Experimental Sciences), Paris, France.

14. Morrison, J.B. (1968). Bioengineering Analysis of Force Actions Transmitted by the Knee Joint, Biomed. Eng., 3, 164-170.

15. Paul, J.P. (1966). The Biomechanics of the Hip Joint and its Clinical Relevance, Proc. R. Soc. Med., **59**, 943-948.

16. Pezzack, J.C., Norman, R.W. and Winter, D.A. (1977). An Assessment of Derivative Determining Techniques Used for Motion Analysis, J. Biomech., **10**, 377-382.

17. Reynolds, H.M. (1985). Personal correspondence.

18. Soutas-Little, R.W., Beavis, G.C., Verstraete, M.C. and Markus, T.L. Analysis of Foot Motion During Running Using a Joint Coordinate System. Submitted for publication to Medicine and Science in Sports and Exercise.

19. Walton, J.S. Close-range Cine-photogrammetry: A Generalized Technique for Quantifying Gross Human Motion, Ph.D. Dissertation, The Pennsylvania State University, May 1981.

20. Weber, Wilhelm and Eduard (1936). Mechanik der menschlichen Gehwerkzeuge (Mechanics of Human Locomotion), Gottingen, Germany.

21. Winter, D.A. (1983). Moments of Force and Mechanical Power in Jogging, J. Biomechanics, **16**, 1, 91-97.

22. Winter, D.A. (1980). Overall Principal at Lower Limb Support During Stance Phase of Gait, J. Biomechanics, 13, 923-927.

23. Winter, D.A., Sidwall, H.G. and Hobson, D.A. (1974). Measurement and Reduction of Noise in Kinematics of Locomotion, J. Biomech., 7, 157-159.